Tectonophysics xxx (2010) xxx–xxx

Contents lists available at ScienceDirect

Tectonophysics

journal homepage: www.elsevier.com/locate/tecto

The origin of the Baydaric microcontinent, Mongolia: Constraints from paleomagnetism and geochronology

Natalia M. Levashova [a,*], Valery M. Kalugin [b], Anatoly S. Gibsher [b], Jessica Yff [c], Alexander B. Ryabinin [b], Joseph G. Meert [c], Shawn J. Malone [c]

[a] Geological Institute, Academy of Science of Russia, Pyzhevsky Lane, 7, Moscow 109017, Russia
[b] Institute of Geology and Mineralogy, Siberian Branch of the Academy of Science of Russia, Koptyug Pr. 3, Novosibirsk 630090, Russia
[c] Department of Geological Sciences, 274 Williamson Hall, Gainesville, FL 32611, USA

ARTICLE INFO

Article history:
Received 9 April 2009
Received in revised form 28 October 2009
Accepted 29 January 2010
Available online xxxx

Keywords:
Central Asia orogenic belt
Geochronology
Paleomagnetism
Mongolia

ABSTRACT

Existing views on the tectonic evolution of the Central Asian orogenic belt (CAOB) are highly controversial and the Neoproterozoic to Cambrian stages of this evolution remain the most enigmatic. However, the views on the Paleozoic evolution of the CAOB crucially depend on these early stages, as different choices of the starting point lead to very dissimilar Paleozoic reconstructions. In this context numerous microcontinents with the Precambrian basement that are included in the mosaic structure of Kazakhstan, Tien Shan, Altai and Mongolia are of particular interest. We undertook a paleomagnetic, geochemical and geochronological study of the Neoproterozoic volcanics from one of these units — the Baydaric microcontinent in Central Mongolia. According to U–Pb (laser ablation) dating the age of the studied Dzabkhan Volcanics is about 770–805 Ma. Thermal demagnetization revealed that most of the studied samples retained a pre-tilting component, whose primary origin is supported by a conglomerate test. These new data, together with available geological information allow us to conclude that about 770–800 Ma ago the Baydaric domain was located at a latitude of 47^{+16}_{-12}° N and belonged to one of the following plates: India, South China, Tarim or Australia.

1. Introduction

Eurasia comprises several major blocks with Precambrian basement, separated by younger mobile belts of Phanerozoic age (Fig. 1a). It can be argued that Eurasia represents a superb natural laboratory for elucidating continental amalgamation leading to the formation of a future supercontinent. The Alpine and Central Asian orogenic belts are the largest in Eurasia. Whereas the former was the locus of Eurasia growth in the Mesozoic and Cenozoic, the latter played the same role through the Neoproterozoic and Paleozoic.

The Central Asian orogenic belt (CAOB) stretches from the Urals to Kazakhstan and Tien Shan to Altai and Mongolia to the Pacific. The central part of the CAOB is located between the European, Siberian, North China, and Tarim platforms (Fig. 1a), and has the most complex tectonic history. Unlike typical inter-continental or peri-continental linear orogenic belts like the Urals, Andes, Appalachians, etc., no prevailing structural trend is observed here. Numerous microcontinents with Precambrian basement and late Neoproterozoic–Early Paleozoic terrigenous clastic or carbonate cover are tectonically juxtaposed with late Neoproterozoic–Early Paleozoic subduction-related volcanic complexes, accretionary wedges and flysch sequences and form mosaic structure.

Existing views on the tectonic evolution of the CAOB are highly controversial. Thus, one can find a slowly evolving flotilla of microcontinents and island arcs (Mossakovsky et al., 1993; Didenko et al., 1994; Filipova et al., 2001), or a gradually coiling serpentine island arc (Şengör and Natal'in, 1996; Yakubchuk et al., 2001, 2002), or an array of larger blocks that consumed surrounding oceans according to models that change from author to author (Puchkov, 2000; Stampfli and Borel, 2002). The co-existence of so many dissimilar models strongly indicates that we lack even first-order knowledge about the paleogeography and kinematics of the CAOB constituents.

It comes as no surprise that the Neoproterozoic–Cambrian stages of CAOB tectonic evolution remain most enigmatic and controversial. However, our views on the Paleozoic evolution of the CAOB crucially depend on these early stages, as different choices of the starting point lead to very dissimilar Paleozoic reconstructions. Two parameters, which vary widely from one model to another, seem to be of major importance: the relative position of Baltica and Siberia in the Neoproterozoic–Cambrian and the origin and subsequent kinematics of Precambrian microcontinents, included in the CAOB. The first problem is definitely beyond the scope of this study, whereas the origin and subsequent kinematics of the microcontinents may provide insights into early history of the Central Asian orogenic belt and in turn impose strong constraints on general style of its tectonic evolution.

* Corresponding author.
E-mail address: namile2007@rambler.ru (N.M. Levashova).

0040-1951/$ – see front matter © 2010 Elsevier B.V. All rights reserved.
doi:10.1016/j.tecto.2010.01.012

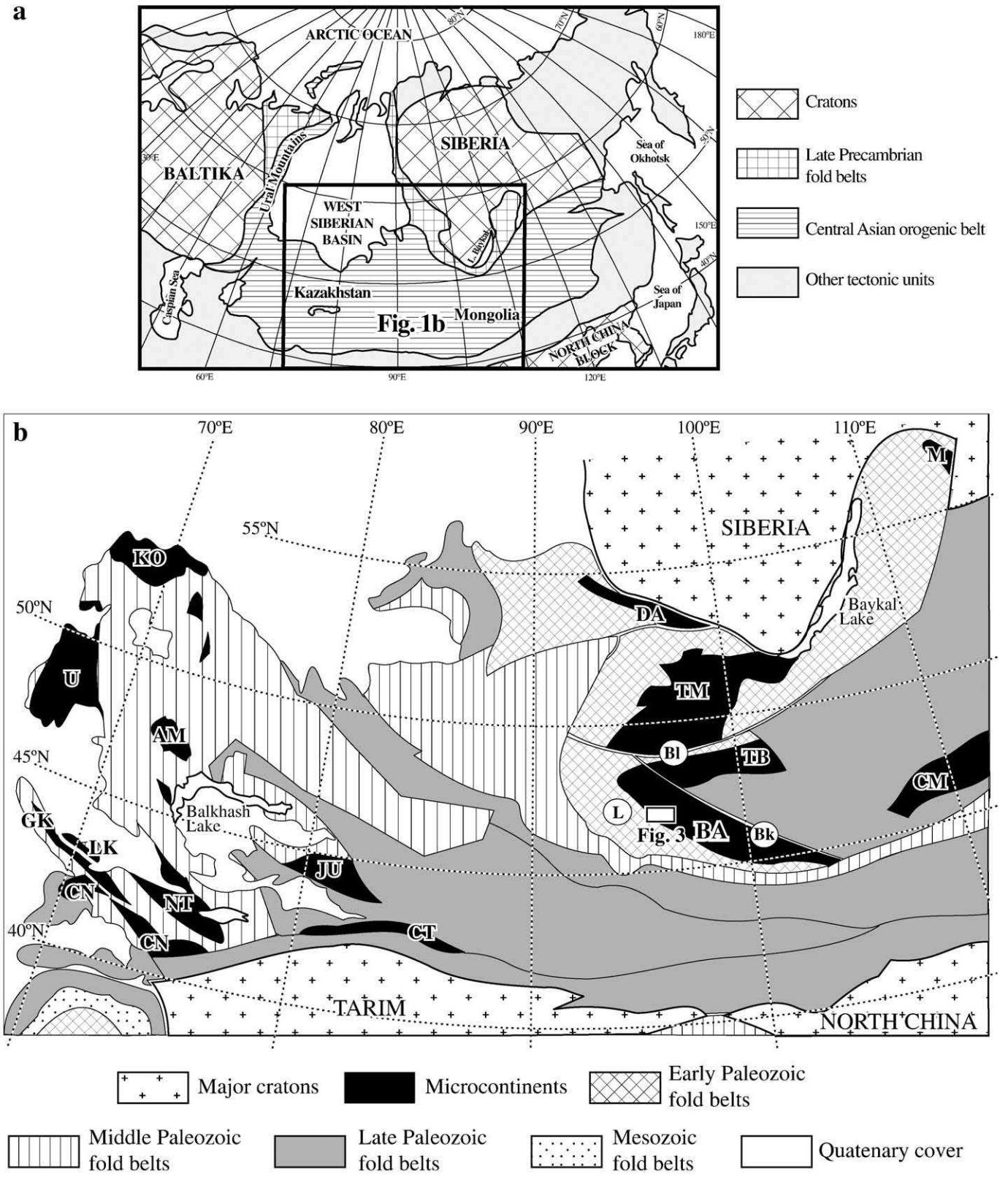

Fig. 1. (a) Location of the Central Asian orogenic belt within Eurasia. (b) Generalized tectonic scheme of the Central Asian orogenic belt and surrounding units (modified after Mossakovsky et al., 1993). Major regional structures are labeled as follows: Bl, Balnay Fault; L, Lake tectonic zone, Bk, Bayankhongor ophiolites. Microcontinents: AM, Aktau-Mointy; CM, Central Mongolian, CN, Chatkal-Naryn; CT, Central Tien Shan; GK, Great Karatau; LK, Lesser Karatau; JU, Jungar; KO, Kokchetav; NT, North Tien Shan; TM, Tuva-Mongolian; U, Ulutau; DA, Derbi-Arzubey; M, Mui; TB, Tarbagatay; BA, Baydaric (or Dzabkhan). The rectangle outlines the area shown in Fig. 3.

The stratigraphic similarities between the Neoproterozoic–Cambrian sections of many of Precambrian microcontinents were noticed decades ago (Ankinovitch, 1962; Zubtsov, 1971). The Neoproterozoic sequences on most microcontinents are represented by volcanic and volcano-sedimentary rocks of rhyolitic and trachyrhyolitic composition. The late Neoproterozoic, mostly terrigeneous rocks are overlain by lower and

Please cite this article as: Levashova, N.M., et al., The origin of the Baydaric microcontinent, Mongolia: Constraints from paleomagnetism and geochronology, Tectonophysics (2010), doi:10.1016/j.tecto.2010.01.012

middle Cambrian carbonates and black shales and late Cambrian–Tremadocian carbonates or siltstones. The two most remarkable marker horizons of the Neoproterozoic–early Paleozoic sections are the late Neoproterozoic glacial diamictites, which are known at one or more stratigraphic levels in many microcontinents (Chumakov, 1978; Korolev and Maksumova, 1984) and the phosphorite layers that occur at the Ediacaran–Cambrian boundary on some of these blocks (Meert and Lieberman, 2008).

Basing on these similarities, many authors had proposed the similar origin of the CAOB microcontinents. According to some of them (Mossakovsky et al., 1993; Didenko et al., 1994; Kheraskova et al., 2003) most microcontinents had rifted from east Gondwana and were moving nearly along the same latitude until the collision with either Siberia or each other, thus forming the hypothetical Paleozoic Kazakhstan continent. In contrast, Zonenshain et al. (1990) had supposed that all these units are of Siberian origin. Şengör and Natal'in (1996) proposed that all these units were moving coherently either with Siberia or Baltica. However, the entire existing hypotheses are highly speculative and the origin of all the microcontinents remains enigmatic.

The most obvious way to improve our understanding of the problem is to obtain a set of paleomagnetic data for the CAOB microcontinents. However, paleomagnetic data are available only for one of the CAOB microcontinents, the Baydaric microcontinent (Fig. 1b) in Central Mongolia. Two members of the Ediacaran–Early Cambrian sedimentary cover of this domain were studied by Evans et al. (1996) and by Kravchinsky et al. (2001). Evans et al. (1996) had interpreted their paleomagnetic result on the Early Cambrian Bayangol Formation as a pre-folding overprint. Kravchinsky et al. (2001) had studied both the Ediacaran–Nemakit–Daldynian Tsagan–Oloom Formation and the Early Cambrian Bayangol Formation. These data are highly scattered and are not supported by any field tests, nevertheless, the authors advocate the primary origin of the result. According to Kravchinsky et al. (2001), the Baydaric microcontinent was located near the equator in Ediacaran–Early Cambrian.

In order to investigate the older rocks from the Baydaric microcontinent we collected Upper Neoproterozoic Dzabkhan Volcanics. We present new U/Pb zircon ages together with the new geochemical and paleomagnetic data. The inclinations obtained in the present study will be compared with the latitudinal positions of most of the continental plates at about 770–800 Ma. This analysis may shed light on the origin of the Baydaric microcontinent.

2. Geological setting and sampling

The Baydaric (or Dzabkhan in some other publications) microcontinent in Central Mongolia is separated from the Tuva-Mongolian microcontinent in the north by the Balnay fault (Fig. 1b). Late Neoproterozoic–Cambrian subduction-related complexes of the Lake (Ozerny in some other publications) tectonic zone and the Bayankhongor Neoproterozoic ophiolite bound the Baydaric microcontinent to the west and south and to the north and east, respectively.

The basement of the Baydaric microcontinent is represented by tonalitic gneisses of the Baydaric Suite (2646 ± 45 U/Pb on zircons (Kozakov et al., 1993)), which is unconformably overlain by metasediments of the Bymbuger Suite (Fig. 2). The basement is intruded by Paleoproterozoic granites (1825 ± 5 U/Pb on zircons (Kotov et al., 1995)) and experienced high-grade metamorphism at 1800–1850 Ma (Khain et al., 2003). Neoproterozoic carbonates and terrigeneous rocks of the Ulzitgol Formation unconformably overlie the basement in the eastern part of the microcontinent.

The Dzabkhan Volcanics (Fig. 2) are mainly represented by andesitic-basalts and andesites in the lower and by felsic volcanics in the upper part of the section, with numerous explosive units, like pyroclastic tuffs and ignimbrites. Locally, lenses of alluvial conglomerates indicate that the volcanics are most probably subaeral. The total thickness of the Dzabkhan Volcanics exceeds 2000 m. The volcanics are

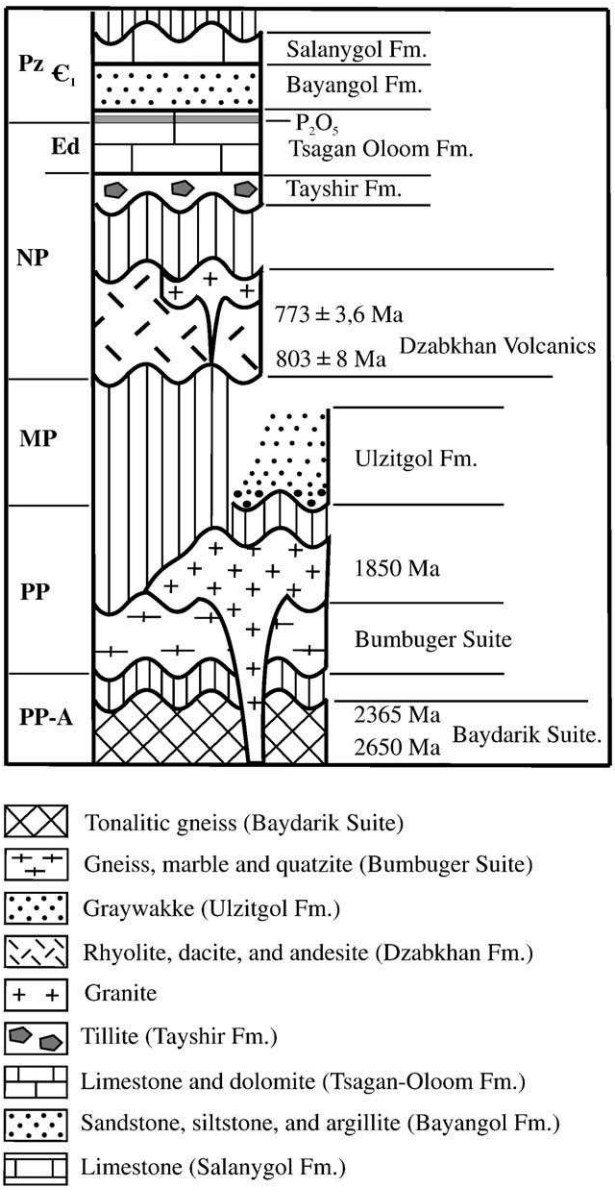

Fig. 2. Schematic stratigraphic column of the Baydaric microcontinent.

intruded by Neoproterozoic tonalites and trondjemites. Locally, the volcanic sequence is overlain conformably and with gradual transition by terrigenous redbeds.

The Dzabkhan volcanic pile is also overlain with both erosional and angular unconformities by late Neoproterozoic–early Cambrian sediments in the Dzabkhan river valley (Fig. 3). Thus, all older complexes were deformed before the late Neoproterozoic (Khomentovsky and Gibsher, 1996). The lowermost part of the sedimentary sequence is represented by tillites of the Tayshir Formation (Lindsay et al., 1996). They are conformably overlain by carbonates of the Nemakit–Daldynian Tsagan–Oloom Formation, that, in turn, are overlain by early Cambrian terrigenous rocks of the Bayangol Formation (Khomentovsky and Gibsher, 1996).

In late Cambrian–early Ordovician time, the subduction-related complexes of the Lake zone (Fig. 1b) were thrust over the shelf of the Baydaric domain. Thrusting and faulting also affected the late Neoproterozoic–early Cambrian sedimentary cover and formed a series of nappes (Khomentovsky and Gibsher, 1996). In Devonian–late Paleozoic time, numerous grabens filled with Devonian to Permian volcanics accumulated on the Baydaric microcontinent. The last phase of tectonism was in the Cenozoic.

Please cite this article as: Levashova, N.M., et al., The origin of the Baydaric microcontinent, Mongolia: Constraints from paleomagnetism and geochronology, Tectonophysics (2010), doi:10.1016/j.tecto.2010.01.012

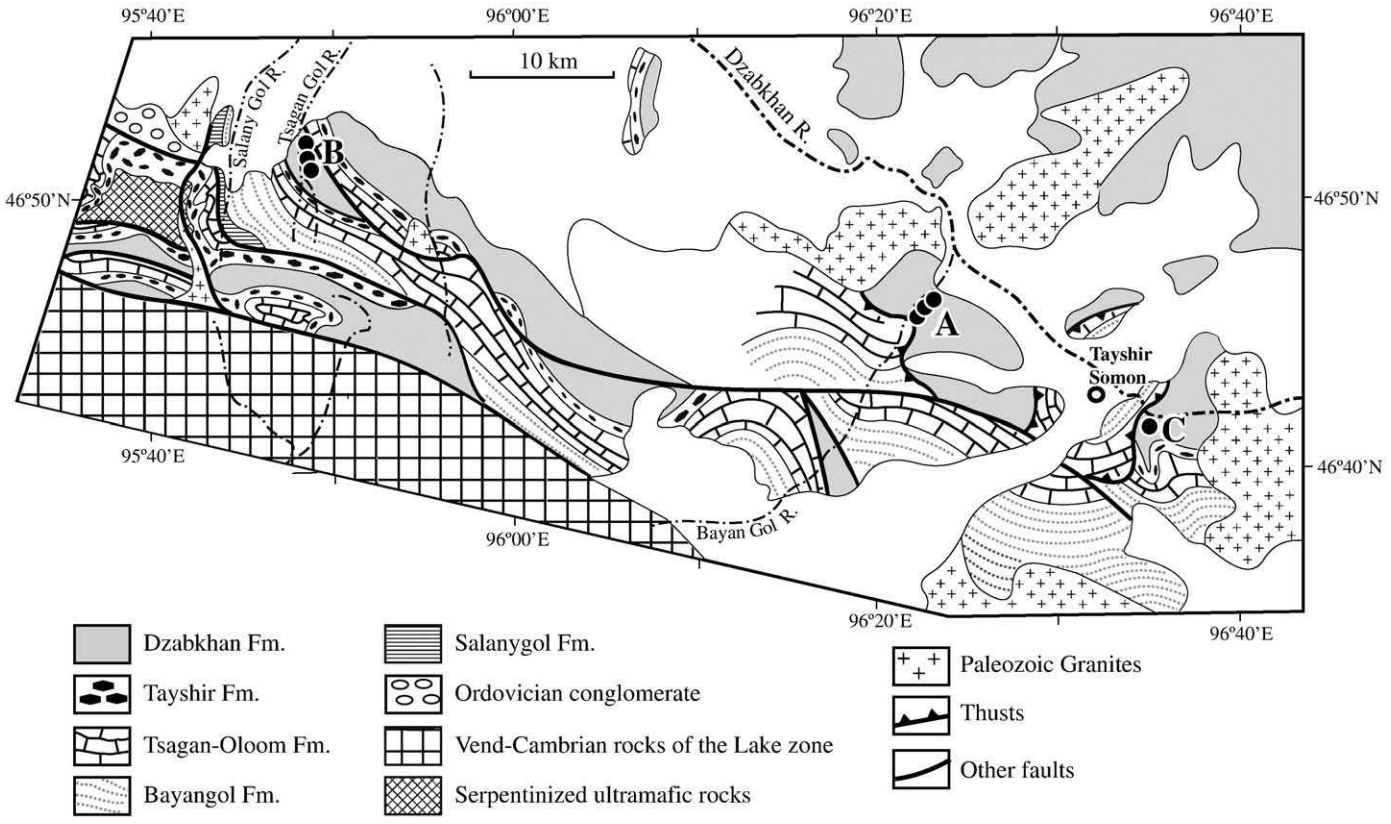

Fig. 3. Schematic geological map of the study area. The sampling localities (solid circles) are labeled as follows: A, the valley of the Bayangol River; B, the valley of the Tsagan-Gol River; and C, the section near the Tayshir-somon.

Our study concentrated on the Neoproterozoic Dzabkhan Volcanics. For a paleomagnetic study, we mainly sampled felsic volcanics and tuffs from three monoclinal sections (Fig. 3). At the locality A we had also sampled 29 lava cobbles from the intraformational conglomerates. The sampled cobbles have the same rhyolite to dacite composition as the underlying and overlying lava flows. Samples for geochemical analysis and U/Pb zircon dating were taken at localities A and B.

3. U–Pb zircon geochronology

Two samples were collected for U–Pb geochronology in this study. Sample B66 (rhyolite) was taken from the upper section of the Dzabkhan Volcanics near Tsagan-Gol river and sample DZ-1 was taken from a rhyolite in the lower part of the section near Bayangol.

3.1. Methods

Zircons were extracted from B66 and DZ-1 using standard mechanical crushing, density, and magnetic separation techniques. The least magnetic zircons were then hand-picked under a binocular scope, mounted in epoxy with the external zircon standard FC-1, and polished to expose the zircons. U–Pb isotopic analyses were conducted at the Department of Geological Sciences (University of Florida) on a Nu Plasma multicollector plasma source mass spectrometer equipped with three ion counters and 12 Faraday detectors. The MC-ICP-MS is equipped with a specially designed collector block for simultaneous acquisition of ^{204}Pb(^{204}Hg), ^{206}Pb and ^{207}Pb signals on the ion-counting detectors and ^{235}U and ^{238}U on the Faraday detectors (see Simonetti et al., 2005). Mounted zircon grains were laser ablated using a New Wave 213 nm ultraviolet beam. During U–Pb analyses, the sample was decrepitated in a He stream and then mixed with Ar-gas for induction into the mass spectrometer. Background measurements were performed before each analysis for blank correction and contributions from ^{204}Hg. Each sample was ablated for ~30 s in an effort to minimize pit depth and fractionation. Data calibration and drift corrections were conducted using the FC-1 Duluth Gabbro zircon standard. Data reduction and correction were conducted using a combination of in-house software and Isoplot (Ludwig, 1999). Additional details can be found in Mueller et al. (2008).

3.2. Results

U–Pb geochronology from samples B66 and DZ-1 reveals concordant Neoproterozoic zircons in the Dzabkhan volcanic sequence (Fig. 4, Table 1). Sample B66, collected near the top of the volcanic sequence, yielded a population of six (~150–200 μm) subhedral zircons that yielded a concordant age of 773.5 ± 3.6 Ma (MSWD = 0.5; Fig. 4a). Sample DZ-1 yielded a smaller population of zircon grains. One grain yielded a concordant age of ~1085 Ma whereas 3 other grains yielded a concordant age of 803.4 ± 8.0 Ma (2σ, MSWD = 0.1; Fig. 4b). Yue (personal communication) reports a SHRIMP age from the top of the Dzabkhan section of 777 ± 6 Ma. We feel the best interpretation of these data is that the Dzabkhan volcanic rocks erupted during the interval from ~805–770 Ma. The older ~1085 Ma age may signify inheritance from the basement.

4. Paleomagnetic studies

4.1. Methods

As a rule, all samples from a separate cooling unit were treated as a site. Paleomagnetic samples were either collected as fist-sized blocks oriented with a magnetic compass or drilled with a portable water-cooled drill and oriented with a magnetic and sun compass.

The collection was studied in the paleomagnetic laboratories of the Geological Institute of the Russian Academy of Sciences in Moscow

Please cite this article as: Levashova, N.M., et al., The origin of the Baydaric microcontinent, Mongolia: Constraints from paleomagnetism and geochronology, Tectonophysics (2010), doi:10.1016/j.tecto.2010.01.012

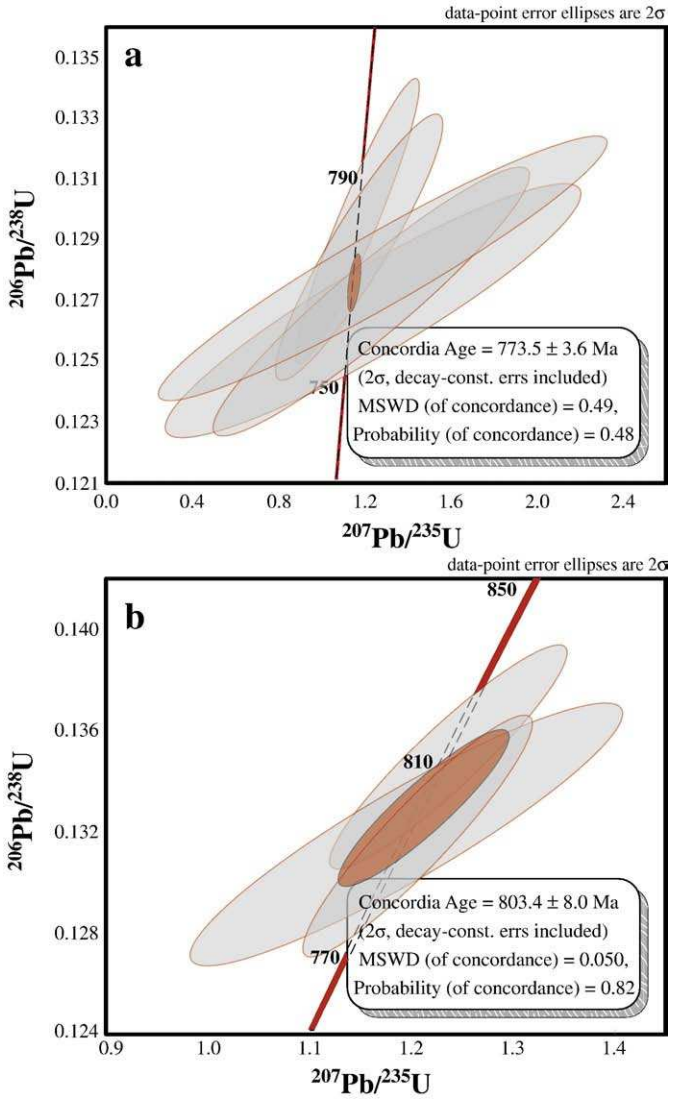

Fig. 4. (a) Results from sample B66 (upper Dzabkhan Volcanics) with a concordant age of 773.5 ± 3.6 Ma and (b) results from sample DZ-1 (lower Dzabkhan Volcanics) with a concordant age of 803.4 ± 8 Ma.

and of the University of Florida in Gainesville. In Moscow, cubic specimens of 8 cm^3 volume were sawed from hand blocks. Specimens were stepwise demagnetized in 15°–20° increments up to 685 °C in a homemade oven with internal residual fields of about 10 nT and measured with a JR-4 spinner magnetometer with a noise level of 0.1 mA m^{-1}. In Gainesville, cylindrical specimens of dimensions 2.2 cm × 2.5 cm were stepwise demagnetized either by thermal or alternating field (AF) methods. AF-treated samples were stepwise demagnetized in 5 mT increments and thermally treated samples were demagnetized in 15°–50 °C up to 685 °C (when required) in an ASC-TD-48 oven and measured on a 2G Enterprises 755R cryogenic magnetometer. No systematic difference was found between the samples that were treated in Moscow or Gainesville, and the data have been pooled.

Demagnetization results were plotted on orthogonal vector diagrams (Zijderveld, 1967). Visually identified linear trajectories were used to determine directions of magnetic components by Principal Component Analysis (PCA), employing a least-squares fit comprising three or more demagnetization steps (Kirschvink, 1980), anchoring the fitting lines to the origin where appropriate. The notation of paleomagnetic components used in description of results is as follows: (1) A low-temperature component A is a remanence removed at initial stages of demagnetization, usually below 300° to 350 °C; (2) An intermediate-temperature component, B, is a remanence that does not show rectilinear decay to the origin and is generally followed by a high-temperature component in the same sample or other samples from the same site; (3) A high-temperature component C is a remanence that shows rectilinear decay to the origin and is generally isolated after removal of B component.

Site-mean directions were computed either using only the PCA-calculated sample directions or combining the latter with remagnetization circles employing the technique of McFadden and McElhinny (1988). Paleomagnetic software written by Jean-Pascal Cogné (Cogné, 2003), Randy Enkin and Stanislav V. Shipunov was used in the analysis.

4.2. Results

The A directions, which were isolated below 300°–350° from most samples (Fig. 5a, b), are well clustered around the present-day field before tilt correction. This remanence is most probably a viscous overprint; since it carries no useful information, it is not further regarded below, and the NRM values are not shown on demagnetization diagrams.

After heating above 200°–350°, both B and C components were isolated from most samples of eleven sites (lava flows) (Fig. 5a–d;

Table 1
LA-ICP-MS data for Dzabkhan Volcanics.

Grain name	$^{207}Pb/^{235}U$	1σ err	$^{206}Pb/^{238}U$	1σ err	$^{207}Pb/^{235}U$ age	1σ err	$^{206}Pb/^{238}U$ age	1σ err
B66-4	1.16465	0.11778	0.12957	0.00194	784	54	785	11
B66-6	1.23796	0.39719	0.12660	0.00173	818	166	768	10
B66-13	1.17473	0.02715	0.12920	0.00201	789	13	783	11
B66-15	1.17153	0.16057	0.12871	0.00181	787	72	781	10
B66-16	1.22852	0.30248	0.12690	0.00183	814	129	770	10
B66-17	1.28073	0.42896	0.12801	0.00180	837	175	776	10
DZ-1	1.20556	0.04637	0.13176	0.00197	803	21	798	11
DZ-2	1.19456	0.08735	0.13183	0.00214	798	40	798	12
DZ-6	1.23607	0.04803	0.13492	0.00183	817	22	816	10
B66-1[a]	2.59925	0.58968	0.12728	0.00205	1300	154	772	12
B66-2[a]	1.55862	0.11049	0.12727	0.00177	954	43	772	10
B66-3[a]	1.32893	0.10239	0.13441	0.00192	858	44	813	11
B66-7[a]	2.00800	0.77909	0.12741	0.00184	1118	234	773	10
B66-8[a]	2.02652	0.15283	0.12716	0.00185	1124	50	772	11
B66-9[a]	1.54539	0.28831	0.12603	0.00179	949	109	765	10
B66-11[a]	1.40322	1.03685	0.13354	0.00187	890	364	808	11
DZ-4[a]	1.38710	0.06962	0.13204	0.00208	883	29	799	12
DZ-5[a]	1.37471	0.08743	0.13135	0.00198	878	37	796	11

Comments: Sample B66 (rhyolite upper section); DZ (rhyolite lower section). 1σ are the s-sigma errors associated with individual ratios or calculated ages.
[a] Grains not used to calculate ages due to high levels of discordance.

Please cite this article as: Levashova, N.M., et al., The origin of the Baydaric microcontinent, Mongolia: Constraints from paleomagnetism and geochronology, Tectonophysics (2010), doi:10.1016/j.tecto.2010.01.012

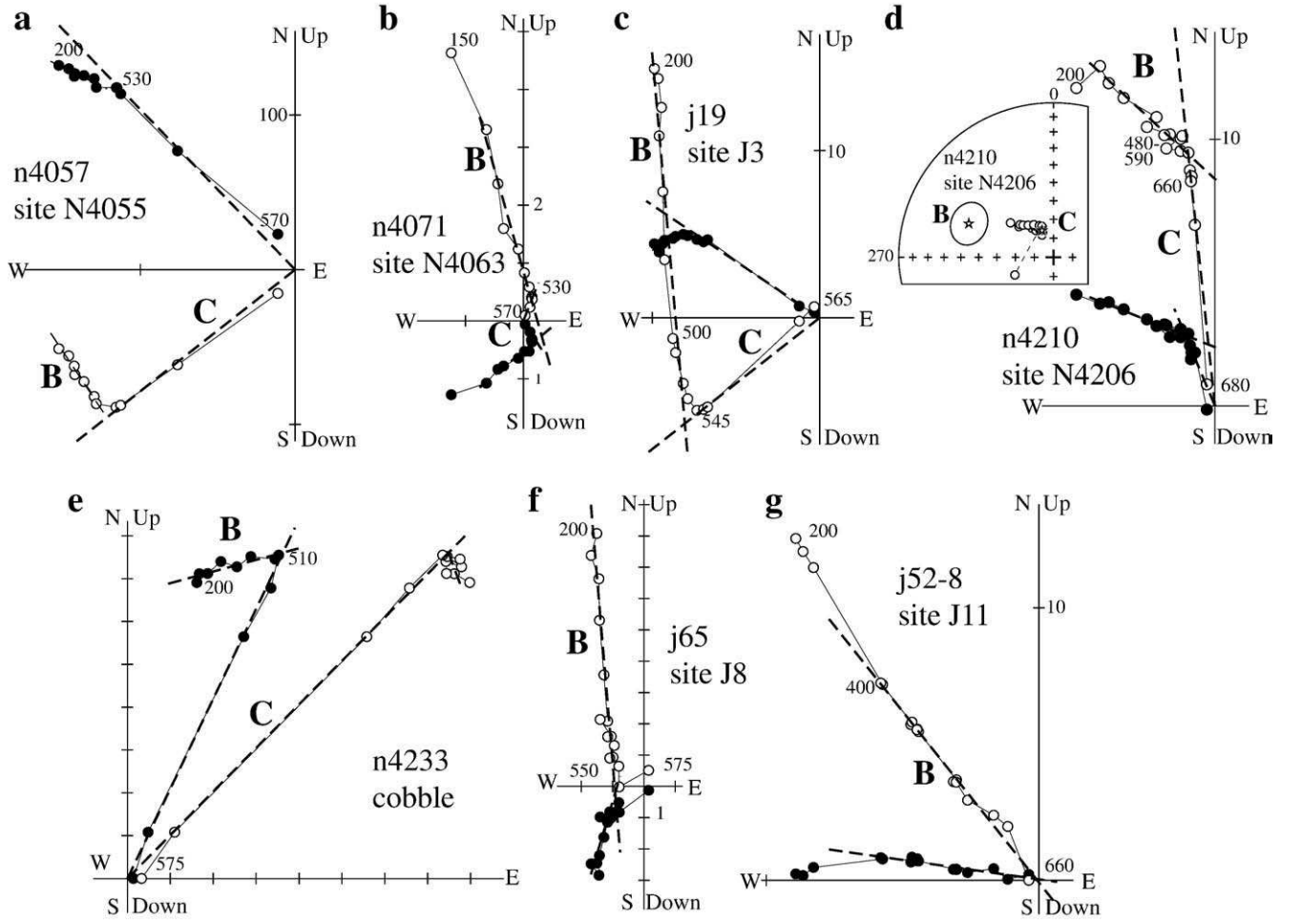

Fig. 5. Representative thermal demagnetization plots of Dzabkhan Volcanics in stratigraphic coordinates: a–d, f–g, dacite and rhyolite flows; e, cobble from an intraformational conglomerate. Full (open) circles represent vector endpoints projected onto the horizontal (vertical) plane. Temperature steps are in degrees Celsius. Magnetization intensities are in mA/m. Dashed lines denote isolated components labeled as in the text. On stereoplot, all symbols are projected onto upper hemisphere, and stars denote the directions of isolated components. For clarity, NRM points are omitted.

Table 2). The B component may be removed from 480 °C to as high as 575 °C. This component is well grouped in all sites (Table 2), and the best grouping of site-means is achieved in geographic coordinates (Dec = 273, Inc = −66, k = 19, a_{95} = 8.2; Fig. 6a).

The C component shows rectilinear decay to the origin and often can be reliably isolated (Fig. 5a, b, c). In cases where proper isolation of this remanence was not achieved, site-mean directions were computed combining the PCA-calculated sample directions with remagnetization circles (McFadden and McElhinny, 1988). The C component is well grouped at all sites (Table 3), and the best site-means grouping is achieved in the stratigraphic coordinates (Fig. 6d), and the fold test (McElhinny, 1964) is positive (Dec = 322, Inc = −65, k = 19, a_{95} = 10.7). One site-mean out of eleven sites is roughly antipodal to the other ten sites (Fig. 6d).

The distributions of site-means of B- and C-component directions partly overlap, after tilt correction in particular, thus raising concern about the validity of their primary/secondary character. For instance, this is the situation at sites N4175 to N4306, where the corresponding site-means look similar. Demagnetization data, however, indicate that both remanences are clearly different (Fig. 5d). Thus these components can be reliably resolved, and the above partial overlap is fortuitous.

The C component resides in both magnetite and hematite in varying proportions (Fig. 7), but its directions do not depend on magnetic mineralogy (Fig. 6). Such a pattern is likely to be due to high-temperature

Table 2
ITC mean directions from Upper Riphean Dzabkhan Volcanics.

S	N/N_0	B	In situ				Tilt-corrected			
			$D°$	$I°$	k	$a_{95}°$	D°	I°	k	$a_{95}°$
N4047	7/7	326/90	229.6	−66.7			169.1	2.5	199	4.3
N4055	5/8	326/90	296.4	−43.8			173.2	−38.9	42	11.9
N4063	6/8	326/90	236.2	−73.9			162.1	−0.1	34	3.6
J1	7/7	326/90	248.8	−76.7			159.0	−2.9	114	5.7
J2	12/12	326/90	230.3	−72.7			163.2	1.7	54	5.9
J3	8/9	326/90	280.2	−84.0			150.3	−4.2	222	3.7
J5	4/7	326/90	287.6	−83.6			150.0	−5.0	262	5.7
J6	11/12	326/90	230.7	−72.5			163.5	1.6	65	5.7
J7	6/7	326/90	235.8	−71.5			164.6	0.1	132	5.8
J8	8/9	326/90	265.5	−84.6			150.7	−2.6	76	6.4
J11	11/15	225/40	263.8	−63.0			181.4	−59.4	27	8.6
N4175	5/7	267/37	276.0	−48.7			323.8	−82.9	83	8.7
N4190	5/8	267/37	286.8	−35.7			313.7	−67.8	41	12.2
N4206	5/7	267/37	286.6	−40.8			322.3	−72.0	47	11.3
N4214	8/8	267/37	267.8	−72.1			86.3	−70.9	44	8.4
N4252	5/7	267/37	310.8	−46.3			1.4	−61.3	31	13.9
N4260	6/8	267/37	279.2	−53.4			5.0	−82.7	106	6.5
Congl.	23/29	267/37	271.8	−63.8			75.9	−78.9	15	8.0
Mean	(18/21)		272.8	−66.2	19	8.2	158.7	−42.8	3	24.7

Comments: S – the site number; N/N_0, number of samples (sites in parenthesis) accepted/studied; B, azimuth of dip/dip angle; D, declination; I, inclination; k, concentration parameter [Fisher, 1953]; a_{95}, radii of confidence circle.

Please cite this article as: Levashova, N.M., et al., The origin of the Baydaric microcontinent, Mongolia: Constraints from paleomagnetism and geochronology, Tectonophysics (2010), doi:10.1016/j.tecto.2010.01.012

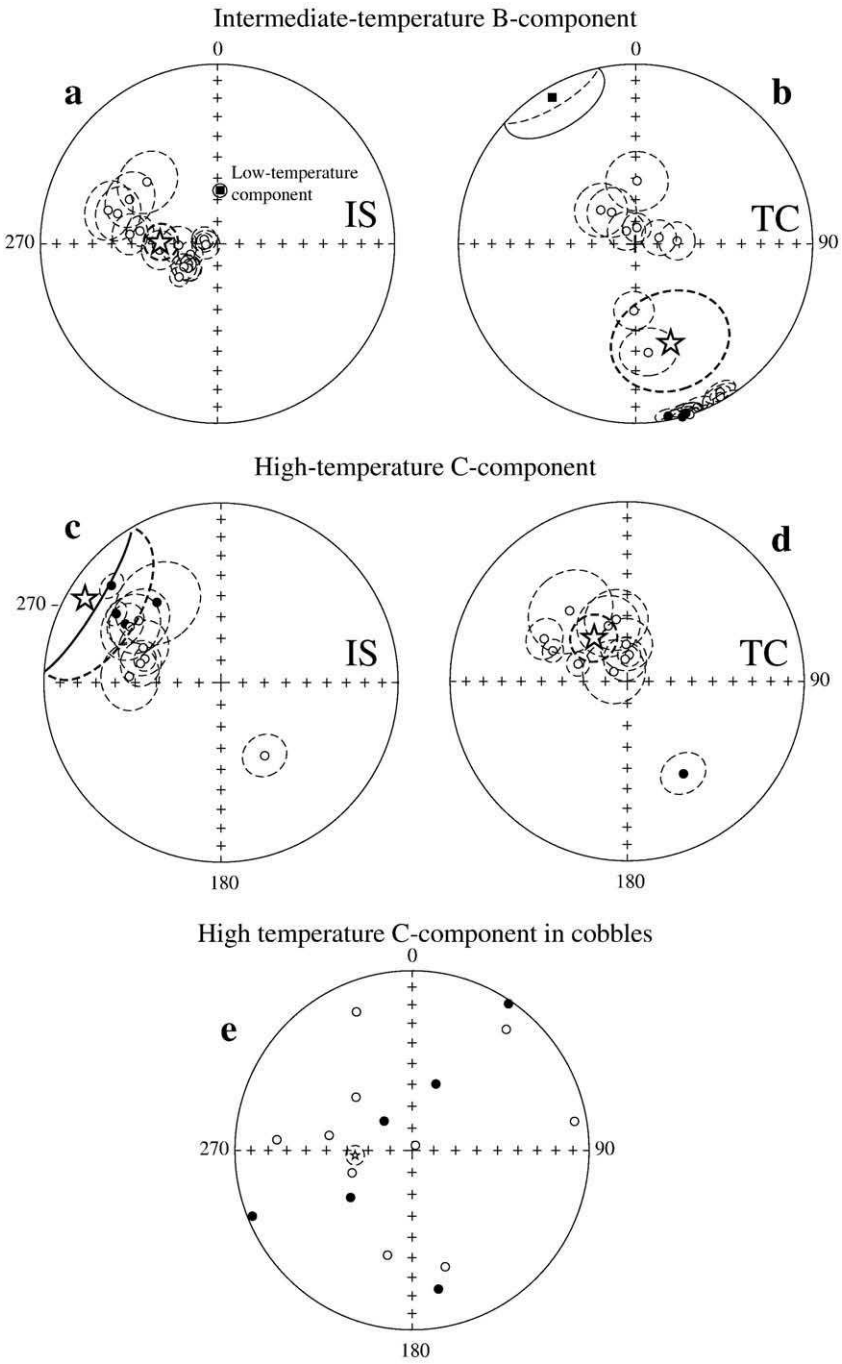

Fig. 6. Stereoplots showing site-mean directions (circles) with associated confidence circles (thin dashed lines) of (a, b) intermediate-temperature component (ITC) and (c, d) of high-temperature component (HTC); (a, c) are in situ (IS) and (b, d) are after tilt correction (TC). Stars are the overall mean directions of the corresponding components with associated confidence circles (thick dashed lines). (e) HTC directions (small dots) from cobbles from an intraformational conglomerate in situ. Star with confidence circle shows the in situ mean direction of the intermediate-temperature component in the cobbles. Solid (open) symbols and solid (dashed) lines are projected onto the lower (upper) hemisphere.

oxidation during emplacement of volcanic units, indicating a primary nature of magnetizations. Fig. 7a–d shows Curie temperature runs for samples that show evidence of remagnetization either present-day field (Fig. 7a) or Late Paleozoic (Fig. 7b). Both samples show large magnetic changes upon heating and cooling. In contrast, samples which passed the fold test show relatively simple Curie temperature results (Fig. 7c, d). Fig. 7c is from a basaltic rock with nearly reversible Curie temperature behavior indicative of magnetite. The large increase in the susceptibility curve shown in Fig. 7d during cooling may indicate exsolution of titanomagnetite.

Two components, B and C, are present in 16 out of 29 lava cobbles from the intraformational conglomerates (Fig. 5e). The remaining cobbles reveal only one component that did not decay to the origin. Although this component does not decay to the origin, the directions isolated from the cobbles match the B component observed in the parent rock. The conglomerate test is positive for the C-component directions (Fig. 6e), as the normalized length of the vector-resultant of 0.20 is less than the 95% critical value of 0.40 of the uniformity test (Mardia, 1972).

The lava samples from sites J2, J8, N4047, and N4214 reveal a single component that does not decay to the origin (Fig. 5f). The presence of a C component can be inferred, but it cannot be isolated because of acquisition of spurious remanence at high temperatures.

Site J11 was collected close to a large early Permian intrusion, and the traces of contact metamorphism are visible in lava samples. These

Please cite this article as: Levashova, N.M., et al., The origin of the Baydaric microcontinent, Mongolia: Constraints from paleomagnetism and geochronology, Tectonophysics (2010), doi:10.1016/j.tecto.2010.01.012

Table 3
HTC mean directions from Upper Riphean Dzabkhan Volcanics.

S	N/N_0	B	In situ				Tilt-corrected			
			D°	I°	k	a_{95}°	D°	I°	k	a_{95}°
N4055	8/8	326/90	311.1	18.9			289.2	−66.1	107	5.4
N4063	7/10	326/90	148.8	−50.6			148.3	39.3	39	9.8
J1	7/7	326/90	301.1	37.0			296.8	−46.5	50	8.8
J3	8/9	326/90	302.9	30.2			292.0	−52.7	129	5.0
J4	7/9	326/90	321.0	42.0			320.5	−47.8	12	19.1
N4175	6/7	267/37	273.8	−47.0			305.6	−82.6	23	14.4
N4190	8/8	267/37	301.2	−39.7			341.1	−63.3	18	14.2
N4198	6/8	267/37	287.0	−52.9			4.6	−78.0	170	5.3
N4206	3/7	267/37	293.7	−50.3			358.4	−73.3	147	12.0
N4252	5/7	267/37	306.6	−41.7			349.9	−61.3	39	14.1
N4260	6/8	267/37	283.2	−51.4			354.6	−80.0	49	9.0
Mean	(11/21)		311.7	−11.0	3	30.1	321.9	−65.0	19	10.7

Comments: All explanations are as for Table 4.

samples reveal a single component, which decays to the origin (Fig. 5g), but its direction coincides with the direction of B component from the other sites and from conglomerates (Fig. 6a). The same is true for sites J6 and J7, where a single component that decays to the origin is isolated.

Combining the B component from the two-component samples, the overprints in conglomerates, the B component from sites N4047, J2, J8 and N4214, as well as the high-temperature directions from sites J6, J7 and J11, we can see that the best site-means grouping is achieved in geographic coordinates (Fig. 6a), and the fold test is negative. Thus, the B component, with a paleomagnetic pole at 31N, 147E, is clearly of secondary origin and postdates folding of the volcanics in the Neoproterozoic and late Cambrian–early Ordovician. Note that there are several early Permian intrusions in the Baydaric microcontinent and in the study area in particular. The lavas from site J11 are visibly affected by such an intrusion, where the lavas are fully remagnetized. Thus it seems very likely that B-component is also of Early Permian age. However, this Permian overprint is ubiquitous in Asia and not wholly unexpected.

In contrast, the positive tilt test, combined with the positive conglomerate test suggests that the C component is of primary origin. This conclusion is further supported by the fact that one site-mean out of eleven sites is roughly antipodal to the other ten (Fig. 6d). The mean inclination of $65° \pm 11°$ indicates that the Baydaric microcontinent was at a latitude of $47^{+16}_{-12}°$ at about 770–805 Ma ago.

5. Geochemical analysis

In the valleys of the Tsagan-Gol and Bayangol rivers (Fig. 8), the Dzabkhan Volcanics form thin to several tens of meters thick lava

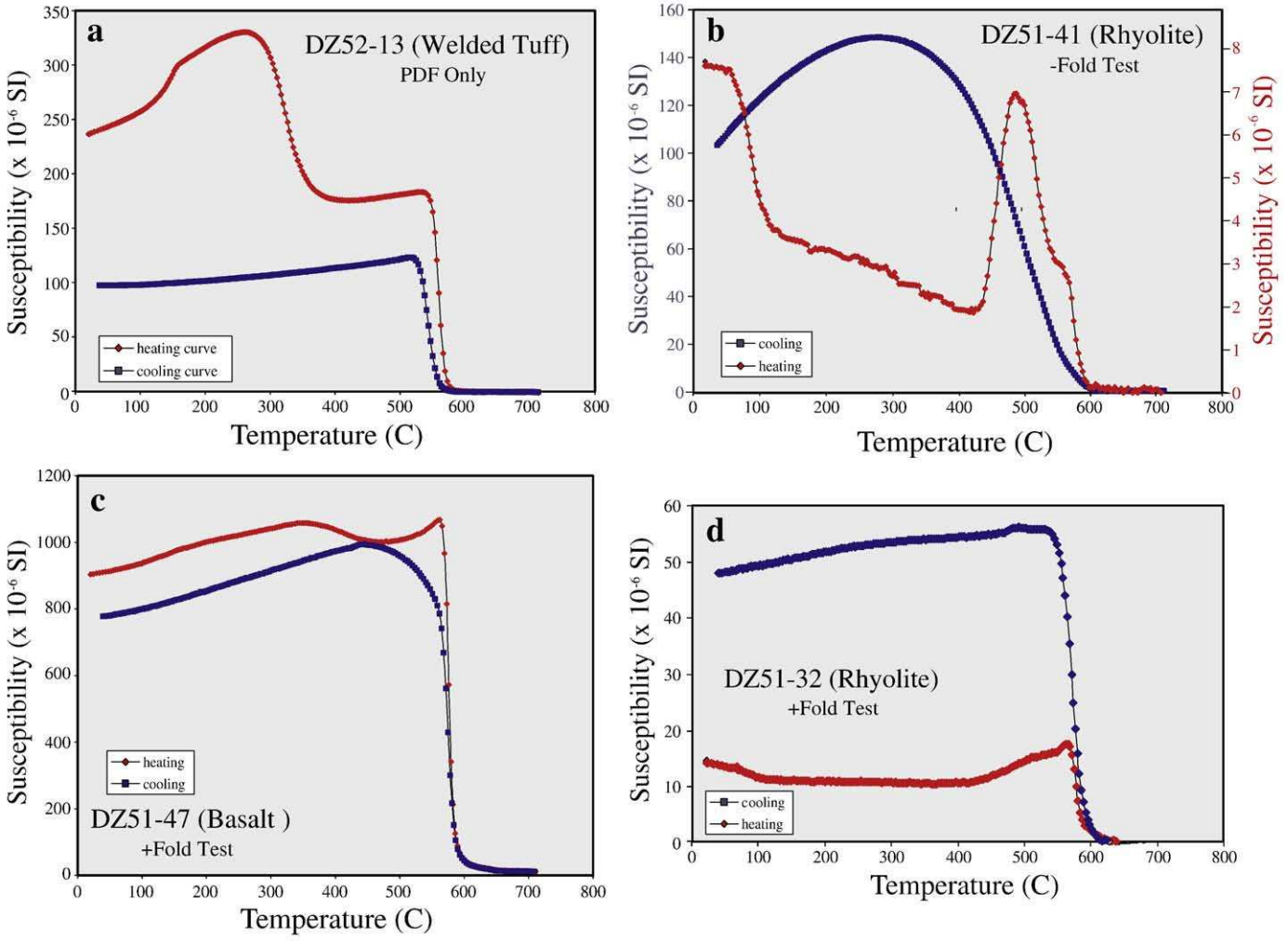

Fig. 7. (a) Temperature-susceptibility plot for welded tuff sample DZ52-13 (Site J13). These samples yielded only a present-day field direction and the sample shows characteristics of pyrrohotite converting to magnetite on heating (b) Temperature-susceptibility plot for rhyolite sample DZ51-41 (Site J5) showing a complex heating curve and alteration of the magnetic mineralogy upon heating (note heating scale is ~1/20 of the cooling susceptibility scale). This sample yielded Group B directions. (c) Temperature-susceptibility plot of basaltic sample DZ51-47 (Site J6) showing nearly reversible heating and cooling curves with a T_c ~ 580 °C. These samples formed part of our Group "C" directions. (d) Temperature-susceptibility plot of rhyolite sample DZ51-32 (Site J1) showing probable exsolution of Ti-magnetite during heating. This sample was part of our Group "C" directions.

Please cite this article as: Levashova, N.M., et al., The origin of the Baydaric microcontinent, Mongolia: Constraints from paleomagnetism and geochronology, Tectonophysics (2010), doi:10.1016/j.tecto.2010.01.012

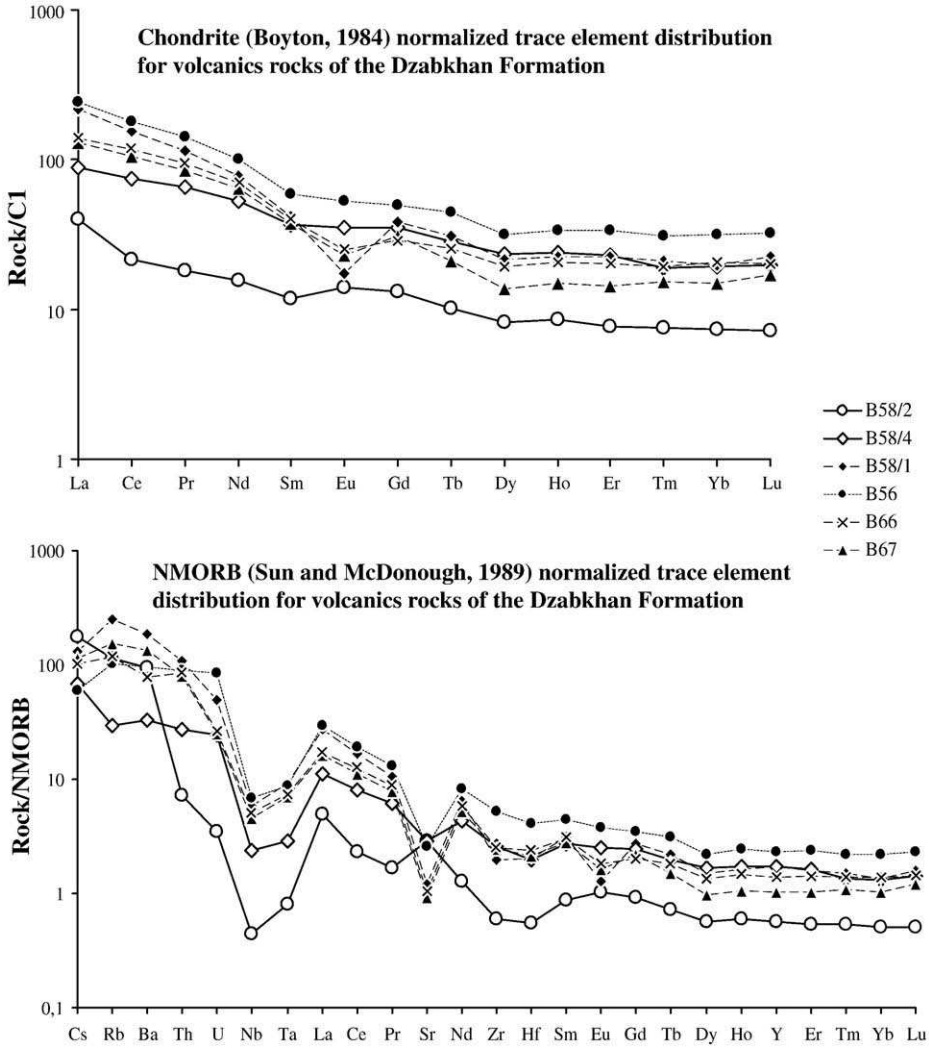

Fig. 8. Chondrite C1 (Boyton, 1984) normalized trace elements distribution (a) and NMORB (Sun and McDonough, 1989) normalized trace elements distribution (b) for the Dzabkhan Volcanics.

flows, tuff layers, small subvolcanic bodies and ignimbrite units mainly of rhyolite to dacite composition (Table 4). The volcanics are cut by numerous felsic dikes 0.1 to several meters wide. Phenocrysts in porphyritic varieties of the rhyolites are represented by quartz, plagioclase and potassium feldspar. Aphanitic rocks have either a felsitic or fluidal texture formed by chains of quartz and feldspar grains. Most felsic rocks are fully crystalline and have felsitic, spherulitic or micropegmatitic texture and have more or less similar compositions (Table 4). Mafic rocks are rare, and only few dolerite dikes less than 1 m wide and basalt flows were found in the studied sections (Table 4). Usually, mafic rocks have a massive structure and ophitic texture. They are mostly crystalline and consist of augite, plagioclase and opaque minerals.

Table 4
Whole-rock major composition of theDzabkhan Formation rocks.

Sample	B58/2	B58/4	B56	B58/1	B66
SiO_2	46.33	46.33	68.49	74.49	77.05
TiO_2	0.76	2.18	0.77	0.12	0.3
Al_2O_3	17.53	15.42	14.45	14.78	16.74
$Fe_2O_3^*$	11.69	17.18	6.57	2.61	0.17
MnO	0.22	0.31	0.19	0.05	0.1
MgO	7.13	4.72	1.11	0.31	0.3
CaO	8.74	5.13	1.69	0.89	0.63
Na_2O	2.42	3.36	2.85	2.8	2.75
K_2O	0.63	0.23	1.07	2.45	0.81
P_2O_5	0.13	0.37	0.4	0.04	<0.03
BaO	0.05	0.03	0.44	0.13	0.05
LOI	4.52	5.43	1.35	0.55	0.69
Total	100.15	100.69	99.38	99.22	99.59

Comments. All major elements were analyzed by XRF (IGM SB RAS, Novosibirsk, Russia). Samples B58/2, B58/4, B56, B58/1 are from the valley of Bayangol river. B58/2 and B58/4 were sampled from the dolerite dykes, B56 from the dacite dike, B58/1 is from the rhyolite lava flow in. Samples B66 and B67 were collected in the valley of the Tsagan-Olom river from two different rhyolite flows.

5.1. Analytical methods

Major elements were determined by XRF in the Institute of Geology and Mineralogy (SB RAS, Novosibirsk). Trace element compositions for bulk rocks were analyzed with a Plasma Quad PQ II Turbo Plus VG ICP-MS instrument (UK) at the Institute of Geochemistry (SB RAS, Irkutsk). Rock chips were powderized and dissolved in acid. Solutions were diluted 1000 times with distilled water with 3% HNO_3. ^{115}In was used as an internal standard with concentration of 10 ppb in solution. Relative errors for each analysis are 5–10%, the lower detection limit is 0.1–1 ppm for each of the analyzed elements. Concentrations were calibrated against international standard rock samples.

Please cite this article as: Levashova, N.M., et al., The origin of the Baydaric microcontinent, Mongolia: Constraints from paleomagnetism and geochronology, Tectonophysics (2010), doi:10.1016/j.tecto.2010.01.012

5.2. Chemical composition

Dzabkhan Volcanics are represented by basalt (SiO_2 up to 46.3 wt.% and alkalies up to 3–3.5 wt.%), dacite (SiO_2 up to 68.49 wt.%, alkalies up to 3.92 wt.%) and rhyolite (SiO_2 up to 74.49 wt.%, alkalies up to 5.25 wt.%). The predominance of Na_2O over K_2O is characteristic for all these rocks.

Both felsic and mafic rocks are enriched in the light rare-earth elements (LREE) ((La/Yb)n = 4.6–7.8, (La/Sm)n = 2.4–4) and large ion lithophile elements (LILE) (Cs, Rb and Ba) (Table 5; Fig. 8). The rare-earth element content in the mafic rocks is less than 100× chondritic values. However, they steadily increase from basalts to rhyolites and reach 150–240× chondritic values for the LREE in the felsic rocks (Fig. 8a). All of the Dzabkhan Volcanics show visible depletion in Nb, Ta, Hf and Zr relative to the LREEs, Ba, Sr, Rb (Fig. 8b). The Nb and Ta minimums points to the subduction-related setting of the Dzabkhan Volcanics.

5.3. Discussion

The Neoproterozoic volcanics of the Dzabkhan Volcanics are usually correlated with Neoproterozoic felsic and bimodal volcanic series of the other CAOB microcontinents (Koksy series from the Ulutau microcontinent, Kainar Formation from the Great Karatau, Bolshoy Naryn Formation from the Central Tien Shan, Altynsyngan Formation from the Aktau-Mointy and Jungar domains, Kopin Formation from the Ili domain, etc.). Different authors interpret the tectonic setting of these rocks in two different ways. Mossakovsky et al. (1993), Kheraskova et al. (1995) and some others hypothesize that all the CAOB microcontinents in Neoproterozoic belonged to the east Gondwana active margin and, therefore, the above listed complexes are subduction-related. However, in many other publications that support the different models of the CAOB evolution (e.g. Ilyin, 1990; Burashnikov and Ruzhentsev, 1993; Khain et al., 2003) all are interpreted as rift volcanics.

It has been widely accepted that Nb and Ta depletions could simply reflect fossil "arc signatures" in the source of the melts, rather than the tectonic environment at the time of the melting. Thus we prefer to abstain from making any definite conclusions on the origin of the Dazabkhan Volcanics.

Table 5
Trace element composition of the Dzabkan Formation volcanics.

Sample	B58/2	B58/4	B56	B58/1	B66	B67
Rock	Basalt	Basalt	Dacite	Rhyolite	Rhyolite	Rhyolite
Cs	1.23	0.48	0.41	0.93	0.72	0.79
Rb	64.17	16.37	58.15	141.18	65.66	87.19
Ba	596.30	209.78	3801.73	1189.36	495.92	852.35
Th	0.86	3.31	10.74	12.85	10.10	9.72
U	0.16	1.14	4.05	2.34	1.25	1.17
Nb	1.04	5.51	15.80	13.64	11.99	10.73
Ta	0.11	0.38	1.17	1.22	0.98	0.92
La	12.42	27.58	74.70	67.83	43.30	40.78
Ce	17.49	60.41	144.87	126.01	93.88	84.17
Pb	26.88	18.00	58.96	13.31	14.56	10.61
Pr	2.19	8.03	17.28	13.99	11.59	10.34
Sr	258.16	256.52	230.30	109.12	92.03	83.77
Nd	9.39	31.60	60.65	46.86	41.94	38.59
Zr	43.91	188.97	387.63	144.25	187.75	178.65
Hf	1.13	4.08	8.48	4.18	4.94	4.36
Sm	2.29	7.13	11.60	8.12	7.88	7.27
Eu	1.04	2.58	3.85	1.29	1.85	1.67
Gd	3.37	9.03	12.93	9.94	7.48	7.97
Tb	0.48	1.33	2.10	1.48	1.20	1.00
Dy	2.61	7.56	10.11	6.90	6.16	4.45
Ho	0.61	1.72	2.44	1.63	1.49	1.07
Y	15.75	48.54	65.26	48.50	38.30	28.44
Er	1.59	4.84	7.07	4.76	4.24	3.01
Tm	0.24	0.62	1.01	0.68	0.62	0.50
Yb	1.53	4.03	6.66	4.15	4.26	3.11
Lu	0.23	0.64	1.05	0.73	0.66	0.55
(La/Yb)n	5.46	4.61	7.57	11.02	6.85	8.85
(La/Sm)n	3.41	2.43	4.05	5.25	3.46	3.53
(Eu/Eu*)n	1.14	0.98	0.96	0.44	0.73	0.67

Comments as for Table 1.

6. Interpretation and discussion

We have already discussed how controversial are the existing views on the tectonic evolution of the CAOB in general and on the seminal late Neoproterozoic–Cambrian stages in particular. Obviously, the better understanding of the origin and subsequent kinematics of the CAOB Precambrian microcontinents may lead to improved understanding of the CAOB evolution. However, the data from at least several domains are needed to reach a significant progress. Analysis of available information on the Baydaric microcontinent should be considered only as the first step, which nevertheless may help to impose some constraints on the views on the early stages of the CAOB evolution.

6.1. Possible origin of the Baydaric microcontinent

All the so far published hypothesis on the origin of the CAOB Precambrian microcontinents (e.g. Zonenshain et al., 1990; Mossakovsky et al., 1993; Didenko et al., 1994; Kheraskova et al., 2003) are based mainly on stratigraphic similarities between the late Neoproterozoic to early Paleozoic sections of the CAOB microcontinents and the coeval sections on the margins of the Tarim, South China and Siberian platforms (Korolev and Maksumova, 1984; Esakova and Zhegallo, 1996; Khain et al., 2003). On the basis of faunal and stratigraphic considerations it was hypothesized that the CAOB microcontinents had rifted either from Siberia (Zonenshain et al., 1990) or from one of the eastern Gondwana blocks (Mossakovsky et al., 1993; Didenko et al., 1994; Kheraskova et al., 2003). Khain et al. (2003) argued that the Kazakhstanian microcontinents had originally belonged to the Tarim plate. The fact that the Baydaric microcontinent (block), as well as many other CAOB microcontinents has Paleoproterozoic basement suggests that it was originally part of a larger continental block.

A commonly accepted Neoproterozoic supercontinent, called Rodinia is hypothesized to have formed at ca. 1100 Ma and broke apart between 800 and 700 Ma (Li et al., 2002, 2008, and references therein), but the locations of separate blocks, on the periphery of the supercontinent in particular, remain controversial; even more contentious are the trajectories of the Rodinia constituents after the supercontinent disintegration. The age of the Dzabkhan Volcanics are coeval with the hypothesized beginning of the Rodinia break-up and thus provide an opportunity to compare our data with existing Rodinia models. We compared the observed paleolatitude with the paleolatitudinal positions of different major blocks using paleomagnetic poles (Table 6) with ages from the 850–750 Ma interval.

At about 770–800 Ma, the Baydaric block was at a latitude of $47^{+16}_{-12}°$, N or S. The southern hemisphere choice for the Baydaric microcontinent places it in the vicinity of the western Gondwana cratons (West Africa, Amazonia, etc.) or in the middle of the Brasiliano Ocean. In the case of the Baydaric microcontinent having been located in the northern hemisphere, it might have belonged to one of the following plates: India Tarim, South China, North China or, may be, Australia, while Siberia and Laurentia were far more to the south at that time (Fig. 9, Table 6). Note, however, that paleomagnetic data are scarce and controversial as exemplified by Australia, where the Hussar pole of Pisarevsky et al. (2007) places this craton at the equator at about 800–760 Ma, while the Walsh tillite pole of Li (2000) of nearly the same age (750–770 Ma) shift Australia to the latitudes, close to the position of the Baydaric block (Fig. 9, Table 6). Thus, the paleoposition of Australia remains highly questionable.

Please cite this article as: Levashova, N.M., et al., The origin of the Baydaric microcontinent, Mongolia: Constraints from paleomagnetism and geochronology, Tectonophysics (2010), doi:10.1016/j.tecto.2010.01.012

Table 6
Selected paleomagnetic poles.

	Rock unit	Age (Ma)	Pole		a_{95}	Lat.	Reference
			(N°)	(E°)			
India/Seychelles							
1	Harohalli dikes	821 ± 12	27	79	9	85 N–71 N	Radhakrishna and Joseph, 1996
2	Malani rhyolites (IND)	761 ± 10	75	71	10	39 N–23 N	Torsvik et al., 2001a
3	Mahe granites (SEY)[e]	755 ± 1	77	23	2	32 N–15 N	Torsvik et al., 2001b
4	Mahe dykes (SEY)[e]	750 ± 3	80	79	16	34 N–18 N	Torsvik et al., 2001b; Hargraves and Duncan, 1990
Australia							
5	Hussar Formation	800–760	62	86	10	3 N–19 S	Pisarevsky et al. (2007)
6	Mundine dykes	755 ± 3	45	135	4	31 N–8 N	Wingate and Giddings (2000)
7	Walsh Tillite	750–770	22	102	14	44 N–19 N	Li (2000)
	Yaltipena Formation[c]	620–630	44	173	8	27 N–5 N	Sohl et al., 1999
	Elatina Formation[c]	600–620	39	186	9	26 N–1 N	Sohl et al., 1999
	Brachina Formation[c]	~580	33	148	16	44 N–20 N	McWilliams and McElhinny, 1980
	Lower Arumbera/Pertataka Formation[c]	~570	44	162	10	30 N–7 N	Kirschvink, 1978
	Upper Arumbera SS[c]	~550	46	157	4	30 N–6 N	Kirschvink, 1978
	Todd River	~530	43	160	7	32 N–9 N	Kirschvink, 1978
South China							
8	Xiaofeng dykes	807 ± 10	14	91	11	~69 N	Li et al., 2004
9	Liantuo Formation	748 ± 12	4	161	13	~37 N	Evans et al., 2000
10	Nantuo Formation[d]	~740	0	151	5	~43 N	Rui and Piper, 1997
	Meishucun Formation[d]	~525	9	31	10	~14 N	Lin et al., 1985
	Tianheban Formation[d]	~511	−7	10	23	~12 S	Lin et al., 1985
	Hetang Formation[d]	~511	−38	16	17	~18 S	Lin et al., 1985
North China							
11	Nanfen Formation	800–780	−16	121	11	~39 N	From Zhang et al., 2006
	Mean pole	~700	−43	107	6	~11 N	From Zhang et al., 2006
	Donjia Formation, Lushan	~650	−61	97	7	~8 S	From Zhang et al., 2006
Tarim							
12	Aksu Dykes	807 ± 12	19	128	6	~43 N	Chen et al., 2004
13	Baiyixi Formation	~740	17	194	4	6 S	Huang et al., 2005
Laurentia							
14	Galeros Formation	780–820	−2	163	6	21 N–25 S	Weil et al. (2004)
15	Wyoming dykes	782 ± 8; 785 ± 8	13	131	4	23 N–36 S	Harlan et al. (1997)
16	Tsezotene sills and dykes	779 ± 2	2	138	5	16 N–34 S	Park et al. (1989)
17	Kwagunt Formation	742 ± 6	18	166	7	41 N–6 S	Weil et al. (2004)
18	Natkusiak Formation	723 ± +4/−2	6	159	6	27 N–20 S	Palmer et al. (1983); Heaman et al. (1992)
19	Franklin dykes	723 ± +4/−2	5	163	5	27 N–19 S	Heaman et al. (1992); Park (1994)
	Long Range Dykes[a]	620–610	19	355	18	34 N–6 S	Murthy et al. (1992)
	Callander complex	575 ± 5	−46	121	6	34 S–81 S	Symons and Chiasson (1991)
	Catochin Basalts-A	564 ± 9	−42	117	9	32 S–77 S	Meert et al. (1994a,b)
	Sept-Iles complex B[b]	564 ± 4	−44	135	5	27 S–74 S	Tanczyk et al. (1987)
Siberia							
20	Karagas Series	850(?)–740	−12	97	10	22 N–8 N	Metelkin et al., 2005 Pavlov et al., in preparation
21	Nersinsky complex	~740	−37	122	11	2 N–19 S	Metelkin et al., 2005 Pavlov et al., in prep.
	Mean pole for V_{2edc}	~560	−35	77	6	3 S–16 S	Shatsillo et al., 2006
	Redkolesnaya Fm.	~550	−61	68	5	30 S–42 S	Shatsillo et al., 2006
	Mean pole for the Nemakit–Daldynian stage	~540	−60	115	7	25 S–41 S	Pavlov et al., in preparation
	Mean pole for Cam_l	~525	−48	151	8	19 S–36 S	Pavlov et al., in preparation
Baltica							
22	Hunnedalen dykes	~848	−41	222	10	59 S–87 S	Walderhaug et al. (1999)
	Egersund dykes	~608	−31	224	15	50 S–81 S	Walderhaug et al. (2007)
	Mean pole	~555	−30	298	10	4 S–31 S	Popov et al. (2002); Iglesia-Llanos et al. (2005); Popov et al. (2005)
	Tornetrask Formation	~535	−56	296	12	24 S–52 S	Torsvik and Rehnstrom (2001)c

Comments: Lat, the range of paleolatitudes, which were occupied by a craton.
Abbreviations: IND, India; SEY, Seychelles.
[a] Recalculated by Hodych et al. (2004).
[b] The Sept-Iles complex "B" direction (after correction for minor tilt — see Symons and Chiasson, 1991) matches other ~570 Ma poles from Laurentia, while "A" direction falls very close to the Cambro-Ordovician segment of the North American APWP (see Meert and Van der Voo, 2001).
[c] Estimated age based on stratigraphic information given in Pisarevsky et al. (2001) and stable isotope calibration given in Walter et al. (2000).
[d] Estimated age based on known isotopic and/or stratigraphic position.
[e] Rotated to India according to Torsvik et al. (2001b).

Please cite this article as: Levashova, N.M., et al., The origin of the Baydaric microcontinent, Mongolia: Constraints from paleomagnetism and geochronology, Tectonophysics (2010), doi:10.1016/j.tecto.2010.01.012

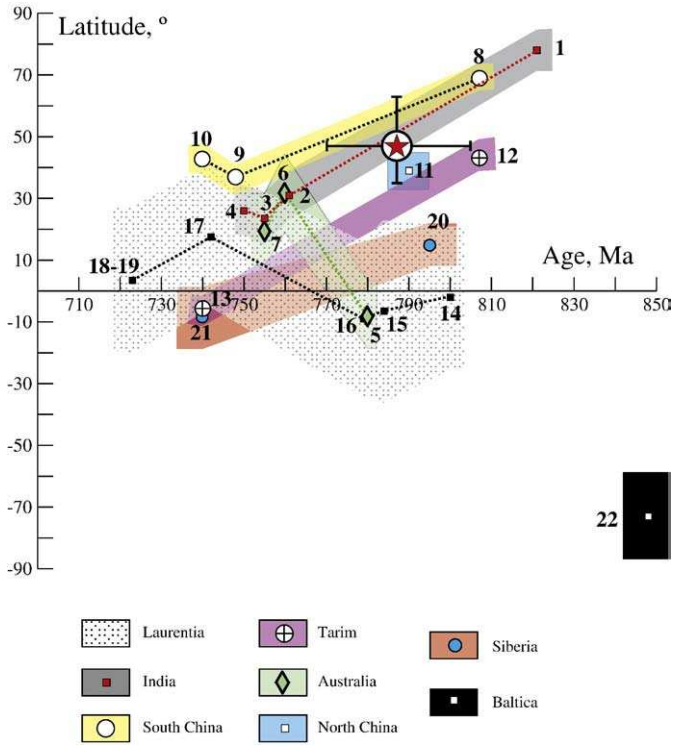

Fig. 9. Paleolatitude versus age plots for major cratons and the observed value for the Dzabkhan volcanics (large encircled star with error bars). For major cratons, the symbols correspond to their centers, while the corresponding bands denote the paleolatitude range (without error limits) covered by this craton. If more than two points are available from a craton, the symbols are connected by thick dashed lines for better visibility. The data are numbered as in Table 6.

Later it will be shown, that faunal and stratigraphic considerations allow to argue that the Baydaric microcontinent was in relatively close proximity to the Tarim, Australia, South China and Siberian plates in the very end of Neoproterozoic — the beginning of Paleozoic. So if the Baydaric block had belonged to one of the northern Rodinian plates at 770–800 Ma, its trajectory to the late Neoproterozoic position was much shorter and less complex than if it had originally belonged to West Africa or Amazonia. Thus, a northern hemispheric choice seems to be more likely, and, in terms of possible paleolatitudinal location, hence the Baydaric block might have belonged either to India, Tarim, South China, Australia, or North China at about 770–800 Ma.

The presence of magmatic rocks that are coeval to the Dzabkhan Volcanics can provide additional constraints regarding its position at the time of eruption. There are no known igneous rocks ranging in age from 1100 to 700 Ma in North China (Lu et al., 2008b), and, most probably, this craton can be excluded from the list of possible 'mother-plates'. Distinguishing between the remaining candidates is difficult to evaluate. These cratons have the basement of the proper Paleoproterozoic age. In Australia the magmatic rocks relatively coeval to the Dzabkhan Volcanics are known in the Adelaide Rift Complex (Veevers, 2004). Neoproterozoic bimodal, anorogenic magmatism in India spans from ca. 860 to 730 Ma (Ashwal et al., 2002; Gregory et al., 2008; Van Lente et al., 2009). The Malani igneous province and coeval Seychelles volcanism is dated as 771 Ma (Torsvik et al., 2001a,b; Gregory et al., 2008; Van Lente et al., 2009). Geological records related to rifting events in the Tarim include mafic dyke swarms, ultramafic–mafic intrusions, alkaline granites, and bimodal volcanic rocks that accumulated in rift basins, all of which were formed between ca. 820 Ma and 740 Ma (Lu et al., 2008a). The rift-related bimodal magmatism of 830–795 Ma and 780–745 Ma age is described at the South China platform (Li et al., 2008).

6.2. Evidence on Baydaric microcontinent history from 800 Ma to the Early Paleozoic

The period between 800 Ma and the early Cambrian (~530 Ma) is a time of a major tectonic re-organization, i.e., the break-up of the supercontinent of Rodinia that was followed by the formation of Gondwana (Meert and Torsvik, 2003). Due to the scarcity of paleomagnetic data, the kinematic of many continental plates is poorly defined for this time interval, and we can only speculate how the CAOB microcontinents moved during this period.

The sedimentary cover overlies the Dzabkhan Volcanics with erosional and angular inconformities and a large time hiatus, up to 200–250 Ma. Thus, there is no evidence on the Baydaric microcontinent evolution during this time. Tentatively, we can conclude that such a long standing above the sea level appears to be more likely for a large landmass than for dispersed minor blocks. If the Dzabkhan Volcanics are the products of continental rifting, one may assume that the Baydaric block (most probably as a part of a much larger landmass) had rifted from a mother plate at the beginning of the Rodinia brake up. There is no geological record of the later rifting event, however, such possibility cannot be excluded.

The stratigraphic similarities between the thick carbonate-clastic sequences of late Neoproterozoic to early Paleozoic age on the CAOB microcontinents and the coeval sections on the margins of the Tarim, South China and Siberian platforms were noticed long ago (Korolev and Maksumova, 1984; Esakova and Zhegallo, 1996; Khain et al., 2003). In particular, there are several marker horizons like Neoproterozoic glacial diamictites (Chumakov, 1978; Korolev and Maksumova, 1984) and phosphorite layers at the Ediacaran–Cambrian boundary (Ilyin, 1990). In the Nemakit–Daldynian (ca. 542–530 Ma) and Tommotian (ca. 530–520 Ma), small shelly fossils of the coeval sections on many CAOB microcontinents, the Tarim craton, the South China block, and the Aldan shield of Siberia have many similar taxa at the family, genus, and even species levels (Esakova and Zhegallo, 1996). In the Atdabanian and Botomian (ca. 520–512 Ma), Siberia, Tarim, South China, and the CAOB microcontinents definitely belonged to the same trilobite province (Repina, 1985). All in all, it is very likely that Baydaric microcontinent (and probably many other CAOB microcontinents) were in close proximity to Siberia, Tarim and South China platforms in the terminal Neoproterozoic–Cambrian. According to the paleomagnetic data of Kravchinsky et al. (2001), the Baydaric microcontinent was located near the equator at that time.

Summarizing, we reach the following conclusions:

A. About 770–800 Ma, the Baydaric block was located at a latitude of $47^{\pm 16^{\circ}}_{12}$ N and belonged to one of the following plates: India, South China, or Tarim,
B. In the Nemakit–Daldynian (ca. 542–530 Ma), the region was dominated by shallow water sedimentation;
C. In the late Neoproterozoic–early Cambrian, the Baydaric microcontinent (and other CAOB microcontinents) was located near the equator in close proximity to Siberia, Tarim and the South China platform.

By the earliest Cambrian (540–530 Ma), Gondwana assembly was largely complete with the exception of small oceanic basins in the region of the Kalahari craton (Fig. 10). Gondwana stretched from the South Pole (South America) to low northern latitudes (Australia). We can hypothesize that, in terminal Neoproterozoic–early Cambrian time, a relatively large shallow sea with a system of island arcs and numerous continental blocks of various size existed at equatorial latitudes to the north of Siberia (Fig. 10). In Nemakit–Daldynian time, small shelly fossils were probably migrating in this hypothetical sea from Siberia to the CAOB microcontinents, Tarim, South China and later to Australia (Repina, 1985). The first archaeocyathid reefs appeared in Siberia within the humid tropical zone in the Tommotian and reached Australia in the middle of the Atdabanian (Zhuravleva, 1981).

Please cite this article as: Levashova, N.M., et al., The origin of the Baydaric microcontinent, Mongolia: Constraints from paleomagnetism and geochronology, Tectonophysics (2010), doi:10.1016/j.tecto.2010.01.012

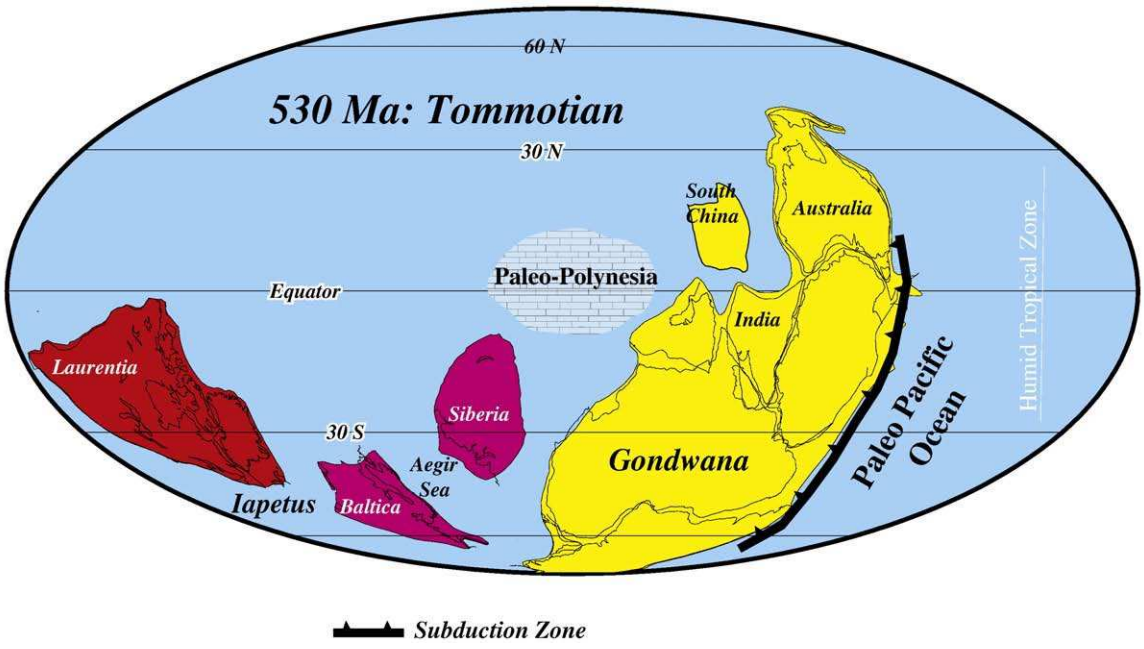

Fig. 10. Paleogeographic reconstruction of Tommotian time (simplified from Fig. 7 in Meert and Lieberman, 2008) showing provisional location of CAOB microcontinents with thick carbonate covers (Paleo-Polynesia).

We must limit ourselves to the above preliminary conclusions here. To further elucidate the early stages of the CAOB tectonic evolution and to logically connect them with the Paleozoic history of this huge mobile belt, more data are needed. In particular, paleomagnetic data on other Precambrian microcontinents are of key importance.

As for subsequent Baydaric microcontinent history, the terrigenous–carbonate sequences are replaced by terrigenous molasses in the Middle Cambrian, thus manifesting the beginning of orogeny. In Late Cambrian–Early Ordovician time, the subduction-related complexes of the Lake zone (Fig. 1b) were thrust on the shelf of the Baydaric block (Khomentovsky and Gibsher, 1996). Thrusting and faulting also affected the Late Neoproterozoic–Early Cambrian sedimentary cover, and a series of nappes was formed (Khomentovsky and Gibsher, 1996). In the end of the Ordovician, the Baydaric block docked to the Siberian periphery (Khain et al., 2003). This event is documented by the episode of high-grade metamorphism and origination of numerous granite intrusions (Yarmoluk et al., 2003).

7. Conclusions

New paleomagnetic and geochronological data on Neoproterozoic volcanics from one of the CAOB microcontinents, the Baydaric block in Central Mongolia, allowed comparing the positions of this domain and major continental blocks for the 770–805 Ma interval. We compared the observed paleolatitude from the Baydaric block with the paleolatitudinal positions of different major blocks using paleomagnetic poles (Table 6) with ages from 850 to 750 Ma interval. The presence of magmatic rocks that are coeval to the Dzabkhan Volcanics can provide additional constraints regarding its position at the time of eruption. Our analysis indicates that the Baydaric domain was located at a latitude of 47^{+16}_{-12}° N at about 800 Ma and belonged to one of the following plates: India, South China, Tarim or Australia.

Acknowledgments

We thank many colleagues from the Geological Institute in Ulaan-Bator, Mongolia, and personally Dr. Tomurhoo, for logistic support of the fieldwork. We warmly acknowledge our colleagues from the Institute of Geology and Mineralogy, Siberian Branch of the Academy of Science of Russia for help in the organization of the fieldwork. We are in debt to Prof. Alfred Kröner for his helpful comments and to Andrey Shatsillo and Vladimir Pavlov for kindly providing us with unpublished results. This study was supported by the Division of Earth Sciences and the Office of International Science and Engineering's Eastern and Central Europe Program of the U.S. National Science Foundation, grant EAR05-08597. Support was also derived from the Russian Foundation of Basic Research, grant 07-05-00021, and Program no. 10 of the Earth Science Division, Russian Academy of Sciences.

References

Ankinovitch, S.G., 1962. The Lower Paleozoic of the vanadium-rich Central Tien-Shan Basin and of the Central Kazakhstan west margin. Nauka KazSSR, Alma-Ata. 189 pp. (in Russian).
Ashwal, L.D., Demaiffe, D., Torsvik, T.H., 2002. Petrogenesis of Neoproterozoic granitoids and related rocks from the Seychelles: evidence for the case of an Andean-type arc origin. Journal of Petrology 43, 45–83.
Boyton, W.V., 1984. Geochemistry of the rare earth elements: meteorite studies. Rare earth element geochemistry. In: Henderson, P. (Ed.), Rare Earth Element Geochemistry. Elsevier, pp. 63–114.
Burashnikov, V.V., Ruzhentsev, S.V., 1993. The Late Riphean–Vendian Sharyngol rift complex (Khasagyn–Nuru Range, West Mongolia). Dokl. RAS 332 (1), 54–57 (in Russian).
Chen, Y., Xu, B., Zhan, S., Li, Y.G., 2004. First mid-Neoproterozoic paleomagnetic results from the Tarim Basin (NW China) and their geodynamic implications. Precambrian Research 133, 271–281.
Chumakov, N.M., 1978. Precambrian Tillites and Tilloides. Nauka, Moscow. 202 pp. (in Russian).
Cogné, J.P., 2003. PaleoMac: a Macintosh application for treating paleomagnetic data and making plate reconstructions. Geochemistry, Geophysics, Geosystems 4 (1), 1007. doi:10.1029/2001GC000227.
Didenko, A.N., Mossakovsky, A.A., Pechersky, D.M., Ruzhentsev, S.V., Samygin, S.G., Kheraskova, T.N., 1994. Geodynamics of Paleozoic oceans of Central Asia. Russian Geology and Geophysics 7–8, 59–75 (in Russian).
Esakova, N.V., Zhegallo, E.A., 1996. The biostratigraphy and fauna of the Early Cambrian in Mongolia. Nauka, Moscow. 270 pp. (in Russian).
Evans, D.A., Zhuravlev, A.Y., Budney, C.J., Kirschvink, J.L., 1996. Palaeomagnetism of the Bayan Gol Formation, western Mongolia. Geological Magazine 133, 487–496.
Evans, D.A.D., Li, Z.X., Kirschvink, J.L., Wingate, M.T.D., 2000. A high-quality mid-Proterozoic paleomagnetic pole from South China, with implications for an Australia–Laurentia connection at 755 Ma. Precambrian Research 100, 213–234.
Filipova, I.B., Bush, V.A., Didenko, A.N., 2001. Middle Paleozoic subduction belts: the leading factor in the formation of the Central Asian fold-and-thrust belt. Russian Journal of Earth Sciences 3, 405–426.
Fisher, R.A., 1953. Dispersion on a sphere. Proceedings of Royal Astronomical Society London, Ser. A 217, 295–305.

Please cite this article as: Levashova, N.M., et al., The origin of the Baydaric microcontinent, Mongolia: Constraints from paleomagnetism and geochronology, Tectonophysics (2010), doi:10.1016/j.tecto.2010.01.012

Gregory, L.C., Meert, J.G., Bingen, B., Pandit, M.K., Torsvik, T.H., 2008. Paleomagnetism and geochronology of the Malani igneous suite, NW India: implications for the configuration of Rodinia and the assembly of Gondwana. Precambrian Research 170, 13–26.
Hargraves, R.B., Duncan, R.A., 1990. Radiometric age and paleomagnetic results from Seychelles dikes. Proceedings of the Ocean Drilling Program: In: Duncan, R.A., et al. (Ed.), Scientific Results Leg, vol. 115, pp. 119–122.
Harlan, S.S., Geissman, J.W., Snee, L.W., 1997. Paleomagnetic and $^{40}Ar/^{39}Ar$ geochronologic data from Late Proterozoic mafic dykes and sills, Montana and Wyoming. USGS Professional Paper 1580, 16 pp.
Heaman, L.M., Le Cheminant, A.N., Rainbird, R.H., 1992. Nature and timing of Franklin igneous events Canada; implications for a late Proterozoic mantle plume and the break-up of Laurentia. Earth and Planetary Science Letters 109, 117–131.
Hodych, J.P., Cox, R.A., Kosler, J., 2004. An equatorial Laurentia at 550 Ma confirmed by Grenvillian inherited zircons dated by LAM ICP-MS in the Skinner Cove volcanics of western Newfoundland: implications for inertial interchange true polar wander. Precambrian Research 129, 93–113.
Huang, B.C., Xu, B., Zhang, C.X., Li, Y.A., Zhu, R.X., 2005. Paleomagnetism of the Baiyisi volcanic rocks (ca.740 Ma) of Tarim Northwest China: a continental fragment of Neoproterozoic Western Australia? Precambrian Research 142, 83–92.
Iglesia-Llanos, M.P., Tait, J.A., Popov, V., Ablamasova, A., 2005. Paleomagnetic data from Ediacaran (Vendian) sediments of the Arkhangelsk region, NW Russia: an alternative APWP of Baltica for the Late Proterozoic–Early Paleozoic. Earth and Planetary Science Letters 240, 732–747.
Ilyin, A.V., 1990. Proterozoic supercontinent, its latest Precambrian rifting, breakup, dispersal into smaller continents, and subsidence of their margins: evidence from Asia. Geology 18, 1231–1234.
Khain, E.V., Bibikova, E.B., Salnikova, E.B., Kroner, A., Gibsher, A.S., Didenko, A.N., Degtyarev, K.E., Fedotova, A.A., 2003. The Palaeo-Asian Ocean in the Neoproterozoic and Early Palaeozoic: new geochronologic data and palaeotectonic reconstructions. Precambrian Research 122, 329–358.
Kheraskova, T.N., Samygin, S.G., Ruzhentsev, S.V., Mossakovsky, A.A., 1995. Upper Riphean active continental margin of the north-east Gondwana. Doklady RAS 342 (5), 661–664.
Kheraskova, T.N., Didenko, A.N., Bush, V.A., Volozh, Y.A., 2003. The Vendian–Early Paleozoic history of the continental margin of eastern Paleogondwana, Paleoasian Ocean, and Central Asian foldbelt. Russian Journal of Earth Sciences 5, 165–184.
Khomentovsky, V.V., Gibsher, A.S., 1996. The Neoproterozoic–Lower Cambrian in northern Gobi-Altay, western Mongolia: regional setting, lithostratigraphy and biostratigraphy. Geological Magazine 133 (4), 371–390.
Kirschvink, J.L., 1978. The Precambrian Cambrian boundary problem; magnetostratigraphy of the Amadeus Basin, central Australia. Geological Magazine 115, 139–150.
Kirschvink, J.L., 1980. The least-square line and plane and the analysis of palaeomagnetic data. Geophysical Journal of the Royal Astronomical Society 62, 699–718.
Korolev, V.G., Maksumova, R.A., 1984. Precambrian Tillites and Tilloides of the Tien-Shan. Ilim, Frunze. 189 pp. (in Russian).
Kotov, A.B., Kozakov, I.K., Bibikova, E.V., Salnikova, E.B., Kirnozova, T.I., Kovach, V.P., 1995. Duration of regional metamorphic episodes in areas of polycyclic endogenic processes: a U–Pb geochronological study. Petrology 3 (6), 567–575 (in Russian).
Kozakov, I.K., Bibikova, E.V., Neymark, L.A., Kirnozova, T.I., 1993. The Baydaric block. In: Rudnik, B.A., Sokolov, Y.M., Filatova, L.I. (Eds.), The Early Precambrian of the Central Asian Fold Belt. St. Petersburg, Nauka, pp. 118–137.
Kravchinsky, V.A., Konstantinov, K.M., Cogne, J.-P., 2001. Paleomagnetic study of Vendian and Early Cambrian rocks of South Siberia and Central Mongolia: was the Siberian platform assembled at this time? Precambrian Research 110, 61–92.
Li, Z.X., 2000. New palaeomagnetic results from the "cap dolomite" of the Neoproterozoic Walsh Tillite, northwestern Australia. Precambrian Research 100, 359–370.
Li, X., Li, Z.X., Zhou, H., Liu, Y., Kinny, P.D., 2002. U–Pb zircon geochronology, geochemistry and Nd isotopic study of Neoproterozoic bimodal volcanic rocks in the Kangdian Rift of South China; implications for the initial rifting of Rodinia. Precambrian Research 113, 133–154.
Li, Z.X., Evans, D.A.D., Zhang, S., 2004. A 90° spin on Rodinia: possible causal links between the Neoproterozoic supercontinent, superplume, true polar wander and low-latitude glaciation. Earth and Planetary Science Letters 220, 409–421.
Li, Z.X., Bogdanova, S.V., Davidson, A., Collins, A.S., De Waele, B., Ernst, R.E., Fitzsimons, I.C.W., Fuck, R.A., Gladkochub, D.P., Jacobs, J., Karlstrom, K.E., Lu, S., Natapov, L.M., Pease, V., Pisarevsky, S.A., Thrane, K., Vernikovsky, V., 2008. Assembly, configuration, and break-up history of Rodinia: a synthesis. Precambrian Research 160, 179–210.
Lin, J.L., Fuller, M.D., Zhang, W.Y., 1985. Paleogeography of the North and South China Blocks during the Cambrian. Journal of Geodynamics 2, 91–114.
Lindsay, J.F., Brasier, M.D., Dorjnamjaa, D., Goldring, R., Kruse, P.D., Wood, R.A., 1996. Facies and sequence controls on the appearance of the Cambrian biota in southwestern Mongolia: implications for the Precambrian–Cambrian boundary. Geological Magazine 133, 417–428.
Lu, S., Li, H., Zhang, C., Niu, G., 2008a. Geological and geochronological evidence for the Precambrian evolution of the Tarim Craton and surrounding continental fragments. Precambrian Research 160, 94–107.
Lu, S., Zhao, G., Wang, H., Hao, G., 2008b. Precambrian basement and sedimentary cover of the North China Craton: a review. Precambrian Research 160, 77–93.
Ludwig, K.R., 1999. Isoplot/Ex version 2.00, a geochronological toolkit for Microsoft Excel. Berkeley Geochronological Center Spec. Publ, 1.
Mardia, K.V., 1972. Statistics of Directional Data. Academic Press, London. 357 pp.
McElhinny, M.W., 1964. Statistical significance of the fold test in palaeomagnetism. Geophysical Journal of the Royal Astronomical Society 8, 338–340.
McFadden, P.L., McElhinny, M.W., 1988. The combined analysis of remagnetization circles and direct observations in palaeomagnetism. Earth and Planetary Science Letters 87, 161–172.
McWilliams, M.O., McElhinny, M.W., 1980. Late Precambrian paleomagnetism in Australia: the Adelaide Geosyncline. Journal of Geology 88, 1–26.
Meert, J.G., Lieberman, B.S., 2008. The Neoproterozoic assembly of Gondwana and its relationship to the Ediacaran–Cambrian radiation. Gondwana Research 14, 5–21.
Meert, J.G., Torsvik, T.H., 2003. The making and unmaking of a supercontinent: Rodinia revisited. Tectonophysics 375, 261–288.
Meert, J.G., Van der Voo, R., 2001. Comment on "New palaeomagnetic result from Vendian red sediments in Cisbaikalia and the problem of the relationship of Siberia and Laurentia in the Vendian" by S. A. Pisarevsky, R. A. Komissarova and A. N. Khramov. Geophysical Journal International 146, 867–870.
Meert, J.G., Van der Voo, R., Payne, T., 1994a. Paleomagnetism of the Catoctin volcanic province: a new Vendian–Cambrian apparent polar wander path for North America. Journal of Geophysical Research 99 (B3), 4625–4641.
Meert, J.G., Hargraves, R.B., Van der Voo, R., Hall, C.M., Halliday, A.N., 1994b. Paleomagnetic and $^{40}Ar/^{39}Ar$ studies of late Kibaran intrusives in Burundi, East Africa: implications for late Proterozoic supercontinents. Journal of Geology 102, 621–637.
Metelkin, D.V., Belonosov, I.V., Gladkochub, D.P., Donskaya, T.V., Mazukabzov, A.M., Stanevich, A.M., 2005. Paleomagnetic directions from Nersa intrusions of the Birusa terrane, Siberian craton as a reflection of tectonic events in the Neoproterozoic. Russian Geology and Geophysics 46, 395–410.
Mossakovsky, A.A., Ruzhentsev, S.V., Samygin, S.G., Kheraskova, T.N., 1993. The Central Asian fold belt: geodynamic evolution and formation. Geotectonics 27 (6), 3–32 (in Russian).
Mueller, P.M., Kamenov, G.D., Heatherington, A.L., Richards, J., 2008. Crustal evolution in the southern Appalachian Orogen: evidence from Hf isotopes in detrital zircons. Journal of Geology 116, 414–422.
Murthy, G., Gower, C., Tubrett, M., Patzold, R., 1992. Paleomagnetism of Eocambrian Long Range dykes and Double Mer Formation from Labrador Canada. Canadian Journal of Earth Sciences 29, 1224–1234.
Palmer, H.C., Baragar, W.R.A., Fortier, M., Foster, J.H., 1983. Paleomagnetism of Late Proterozoic rocks, Victoria Island, Northwest Territories, Canada. Canadian Journal of Earth Sciences 20, 1456–1469.
Park, J.K., 1994. Palaeomagnetic constraints on the position of Laurentia from middle Neoproterozoic to Early Cambrian times. Precambrian Research 69, 95–112.
Park, J.K., Norris, D.K., Larochelle, A., 1989. Paleomagnetism and the origin of the Mackenzie Arc of northwestern Canada. Canadian Journal of Earth Sciences 26, 2194–2203.
Pavlov, V.E., Kravchinsky, V.A., Shatsillo, A.V., Petrov, P. Yu., Paleomagnetism of the Upper Riphean rocks of the Turukhansk, Olenek and Uda Cis-Sayan regions: implications to Neoproterozoic drift of the Siberian platform (in preparation).
Pisarevsky, S.A., Li, Z.X., Grey, K., Stevens, M.K., 2001. A palaeomagnetic study of Empress 1A, a stratigraphic drillhole in the Officer Basin: evidence for a low-latitude position of Australia in Neoproterozoic. Precambrian Research 110, 93–108.
Pisarevsky, S.A., Wingate, M.T.D., Stevens, M.K., Haines, P.W., 2007. Paleomagnetic results from the Lancer-1 stratigraphic drill hole, Officer Basin, Western Australia, and implications for Rodinia reconstructions. Australian Journal of Earth Sciences 54, 561–572.
Popov, V., Iosifidi, A., Khramov, A., Tait, J., Bachtadze, V., 2002. Paleomagnetism of Upper Vendian sediments from the Winter Coast, White Sea region, Russia: implications for the paleogeography of Baltica during Neoproterozoic times. Journal of Geophysical Research 107, 2315. doi:10.1029/2001JB001607.
Popov, V., Khramov, A., Bachtadze, V., 2005. Paleomagnetism, magnetic stratigraphy and petromagnetism of the Upper Vendian sedimentary rocks in the sections of the Zolotitsa River and in the Verkhotina Hole, Winter Coast of the White Sea, Russia. Russian Journal of Earth Sciences 7, 1–29.
Puchkov, V.N., 2000. Paleogeodynamics of the Southern and Middle Urals. Dauria, Ufa. 146 pp. (in Russian).
Radhakrishna, T., Joseph, M., 1996. Late Precambrian (850–800 Ma) paleomagnetic pole for the south Indian Shield from the Harohalli alkaline dykes; geotectonic implications for Gondwanareconstructions. Precambrian Research 80, 77–87.
Repina, L.N., 1985. The paleobiogeography of the Early Cambrian seas based on trilobites, biostratigraphy and biogeography of the Paleozoic in Siberia. Publishing House of the Institute of Geology and Geophysics of the Siberian Branch. Russian Academy of Sciences, Novosibirsk, pp. 5–15 (in Russian).
Rui, Z.Q., Piper, J.D.A., 1997. Paleomagnetic study of Neoproterozoic glacial rocks of the Yangzi Block: paleolatitudes and configuration of South China in the late Proterozoic supercontinent. Precambrian Research 85, 173–199.
Şengör, A.M.C., Natal'in, B.A., 1996. Paleotectonics of Asia: fragments of a synthesis. In: Yin, A., et al. (Ed.), The Tectonic Evolution of Asia. Cambridge University Press, Cambridge, pp. 486–640.
Shatsillo, A.V., Didenko, A.N., Pavlov, V.E., 2006. Paleomagnetism of Vendian deposits of the Southwestern Siberian platform. Russian Journal of Earth Sciences 8, ES2003. doi:10.2205/2005ES000182 (in Russian).
Simonetti, A., Heaman, L.M., Hartlaub, R.P., Creaser, R.A., MacHattie, T.G., Bohm, C., 2005. U–Pb zircon dating by laser ablation-MC-ICP-MS using a new multiple ion counting Faraday collector array. Journal of Analytical Atomic Spectroscopy 20, 677–686.
Sohl, L.E., Christie-Blick, N., Kent, D.V., 1999. Paleomagnetic polarity reversals in Marinoan (ca 600 Ma) glacial deposits of Australia: implications for the duration of low-latitude glaciation in Neoproterozoic time. Geological Society of America Bulletin 111, 1120–1139.
Stampfli, G.M., Borel, G.D., 2002. A plate tectonic model for the Paleozoic and Mesozoic constrained by dynamic plate boundaries and restored synthetic oceanic isochrons. Earth and Planetary Science Letters 196, 17–33.
Sun, S.-S., McDonough, W.F., 1989. Chemical and isotopic systematics of oceanic basalts; implication for mantle composition and pricesses. Magmatism in the ocean basins. Geological Society of London, Special Publication 313–345.
Symons, D.T.A., Chiasson, A.D., 1991. Paleomagnetism of the Callander Complex and the Cambrian apparent polar wander path for North America. Canadian Journal of Earth Sciences 28, 355–363.

Please cite this article as: Levashova, N.M., et al., The origin of the Baydaric microcontinent, Mongolia: Constraints from paleomagnetism and geochronology, Tectonophysics (2010), doi:10.1016/j.tecto.2010.01.012

Tanczyk, E.I., Lapointe, P., Morris, W.A., Schmidt, P.W., 1987. A paleomagnetic study of the layered mafic intrusions at Sept-Iles, Quebec. Canadian Journal of Earth Sciences 24, 1431–1438.

Torsvik, T.H., Rehnstrom, E.F., 2001. Cambrian paleomagnetic data from Baltica: implications for true polar wander and Cambrian paleogeography. Journal of the Geological Society of London 158, 321–329.

Torsvik, T.H., Carter, L.M., Ashwal, L.D., Bhushan, S.K., Pandit, M.K., Jamtveit, B., 2001a. Rodinia refined or obscured: palaeomagnetism of the Malani igneous suite (NW India). Precambrian Research 108, 319–333.

Torsvik, T.H., Ashwal, L.D., Tucker, R.D., Eide, E.A., 2001b. Neoproterozoic geochronology and palaeogeography of the Seychelles microcontinent: the India link. Precambrian Research 110, 47–59.

Van Lente, L.D., Ashwal, M.K., Pandit, S.A., Bowring, Torsvik, T.H., 2009. Neoproterozoic hydrothermally altered basaltic rocks from Rajasthan, northwest India: implications for late Precambrian tectonic evolution of the Aravalli Craton. Precambrian Research 170, 202–222.

Veevers, J.J., 2004. Gondwanaland from 650–500 Ma assembly through 320 Ma merger in Pangea to 185–100 Ma breakup: supercontinental tectonics via stratigraphy and radiometric dating. Earth Science Reviews 68, 1–132.

Walderhaug, H.J., Torsvik, T.H., Eide, E.A., Sundvoll, B., Bingen, B., 1999. Geochronology and paleomagnetism of the Hunnedalen dykes, SW Norway: implications for the Sveconorwegian apparent polar wander loop. Earth and Planetary Science Letters 169, 71–83.

Walderhaug, H.J., Torsvik, T.H., Halvorsen, E., 2007. The Egersund dykes (SW Norway): a robust Early Ediacaran (Vendian) palaeomagnetic pole from Baltica. Geophysical Journal International 168, 935–948.

Walter, M.R., Veevers, J.J., Calver, C.R., Gorjan, P., Hill, A.C., 2000. Dating the 840–544 Ma Neoproterozoic interval by isotopes of strontium, carbon and sulfur in seawater, and some interpretative models. Precambrian Research 100, 371–432.

Weil, A.B., Geissman, J.W., Van der Voo, R., 2004. Paleomagnetism of the Neoproterozoic Chuar Group, Grand Canyon Supergroup, Arizona: implications for Laurentia's Neoproterozoic APWP and Rodinia break-up. Precambrian Research 129, 71–92.

Wingate, M.T.D., Giddings, J.W., 2000. Age and paleomagnetism of the Mundine Well dyke swarm, western Australia: implications for an Australia–Laurentia connection at 750 Ma. Precambrian Research 100, 335–357.

Yakubchuk, A.S., Seltmann, R., Shatov, V.V., Cole, A., 2001. The Altaids: tectonic evolution and metallogeny. Society of Economic Geologists Newsletter 46, 7–14.

Yakubchuk, A., Cole, A., Seltmann, R., Shatov, V.V., 2002. Tectonic setting, characteristics, and regional exploration criteria for gold mineralization in the Altaid tectonic collage: the Tien Shan province as a key example. Society of Economic Geologists, Special Publications 9, 177–201.

Yarmoluk, V.V., Kovalenko, V.I., Kovach, V.P., Kozakov, I.K., Kotov, A.B., Salnikova, E.B., 2003. The geodynamics of the formation of the Caledonian structures of the Central Asian fold belt. Doklady RAS 389, 1–6 (in Russian).

Zhang, S., Li, Z.X., Wu, H., 2006. NewPrecambrian palaeomagnetic constraints on the position of the North China Block in Rodinia. Precambrian Research 144, 213–238.

Zijderveld, J.D.A., 1967. AC demagnetization of rocks: analysis of results. In: Collinson, D.W., et al. (Ed.), Methods in Paleomagnetism. Elsevier, Amsterdam, pp. 254–286.

Zonenshain, L.P., Kuzmin, M.I., Natapov, L.M., 1990. Geology of the USSR: a plate-tectonic synthesis: Amer. Geophys. Union, Washington, D.C. Geodynamics Series, 21. 242 pp.

Zubtsov, E.L., 1971. The Late Precambrian Ulutau–Tien-Shan tillite complex. Moscow State University, Moscow. 129 pp. (in Russian).

Please cite this article as: Levashova, N.M., et al., The origin of the Baydaric microcontinent, Mongolia: Constraints from paleomagnetism and geochronology, Tectonophysics (2010), doi:10.1016/j.tecto.2010.01.012